DOE/NASA/1087–1
NASA CR–189126

Three–Dimensional Modeling of Diesel Engine Intake Flow, Combustion and Emissions

R.D. Reitz and C.J. Rutland
University of Wisconsin–Madison
Madison, Wisconsin

March 1992

Prepared for
NATIONAL AERONAUTICS AND SPACE ADMINISTRATION
Lewis Research Center
Under Grant NAG3–1087

for
U.S. DEPARTMENT OF ENERGY
Office of Conservation
Transportation Systems

DISCLAIMER

Printed in the United States of America

Available from
National Technical Information Service
U.S. Department of Commerce
5285 Port Royal Road
Springfield, VA 22161

NTIS price codes[1]
Printed copy: A04
Microfiche copy: A01

[1]Codes are used for pricing all publications. The code is determined by the number of pages in the publication. Information pertaining to the pricing codes can be found in the current issues of the following publications, which are generally available in most libraries: *Energy Research Abstracts (ERA); Government Reports Announcements* and Index (*GRA* and I); *Scientific and Technical Abstract Reports (STAR);* and publication, NTIS-PR-360 available from NTIS at the above address.

DOE/NASA/1087-1
NASA CR–189126

Three–Dimensional Modeling of Diesel Engine Intake Flow, Combustion and Emissions

R.D. Reitz and C.J. Rutland
University of Wisconsin–Madison
Madison, Wisconsin

March 1992

Prepared for
National Aeronautics and Space Administration
Lewis Research Center
Cleveland, Ohio 44135
Under Grant NAG3–1087

for
U.S. DEPARTMENT OF ENERGY
Office of Conservation
Transportation Systems
Washington, D.C. 20545
Under Interagency Agreement DE–A101–91CE50306

Three-Dimensional Modeling of Diesel Engine Intake Flow, Combustion and Emissions

DOE/NASA-Lewis
University of Wisconsin Grant*

October, 1991

Principal Investigators: R.D. Reitz and C.J. Rutland
Engine Research Center
Department of Mechanical Engineering
University of Wisconsin-Madison

*Research sponsored by the U.S. Department of Energy, Assistant Secretary of Conservation and Renewable Energy, Office of Transportation Technologies, administered by NASA-Lewis under Grant number NAG 3-1087, William Wintucky Grant Monitor.

Report Period 10/89 - 9/91

ABSTRACT

A three-dimensional computer code (KIVA) is being modified to include state-of-the-art submodels for diesel engine flow and combustion: spray atomization, drop breakup/coalescence, multi-component fuel vaporization, spray/wall interaction, ignition and combustion, wall heat transfer, unburned HC and NOx formation, soot and radiation and the intake flow process.

Improved and/or new submodels which have been completed are: wall heat transfer with unsteadiness and compressibility, laminar-turbulent characteristic time combustion with unburned HC and Zeldo'vich NOx, and spray/wall impingement with rebounding and sliding drops. Results to date show that adding the effects of unsteadiness and compressibility improves the accuracy of heat transfer predictions; spray drop rebound can occur from walls at low impingement velocities (e.g., in cold-starting); larger spray drops are formed at the nozzle due to the influence of vaporization on the atomization process; a laminar-and-turbulent characteristic time combustion model has the flexibility to match measured engine combustion data over a wide range of operating conditions; and, finally, the characteristic time combustion model can also be extended to allow predictions of ignition.

The accuracy of the predictions is being assessed by comparisons with available measurements. Additional supporting experiments are also described briefly. To date, comparisons have been made with measured engine cylinder pressure and heat flux data for homogeneous charge, spark-ignited and compression-ignited engines, and also limited comparisons for diesel engines. The model results are in good agreement with the experiments.

CONTENTS

INTRODUCTION

A detailed understanding of diesel engine combustion is required in order to work effectively at improving performance and reducing emissions while not compromising fuel economy. The objective of this research is to apply advanced modeling techniques to study the influence of in-cylinder processes on efficiency and pollutant emissions. The three-dimensional code, KIVA [1,2], has been selected for use since it is the most developed of available codes.

State-of-the-art submodels for the important physical processes in diesel combustion are being included in KIVA as part of the research effort. This report summarizes progress to date on models for wall heat transfer, fuel drop vaporization, spray vaporization, atomization, ignition and the intake flow process. Future activities under the grant are also described briefly .

Close contact is being maintained with engine industries during the course of the research. This includes participation in DOE diesel engine working group meetings[1]. In addition, technology has been transferred directly to industry (e.g., we have already made the FORTRAN subroutines listed in Appendix 3 of this proposal available to the Software Development Group, Engine Division, Caterpillar Inc.).

Other activities that have helped the research effort include our pro-active role in the formation and organization of the KIVA users group (which currently numbers about 80 organizations in the U.S. - see Appendix 1). This activity has had the additional benefit of keeping us informed of code enhancements and new developments elsewhere in the user community. Improvements are being made to the KIVA code itself at the Los Alamos National Laboratories. We have been able to take advantage of their enhancements by ensuring that our submodels are transportable in the form of subroutines (e.g., Appendix 3).

BACKGROUND

The diesel engine is the leading heavy-duty power plant because of its superior energy efficiency. However, because of environmental concerns, proposed federal emission standards require reductions in both nitric oxides (NOx) and particulates for heavy-duty diesel engines. A detailed understanding of combustion is required in order to work effectively at reducing these by-products of combustion *within* the engine cylinder, while still not compromising engine fuel economy. Alternative methods of

---

[1]Prof. Reitz gave the presentations 'Modeling Diesel Engine Spray Evaporation and Combustion' at the Spring 1991 DOE Diesel Group Meeting, Cummins Engine Company, Indiana, May 2, 1991, and '3-D Modeling of Diesel Spray Vaporization and Combustion,' Fall 1991 DOE Diesel Group Meeting, Pennsylvania State University, October 23, 1991.

controlling emissions *outside* of the engine cylinder by means of particulate traps and catalysts are not appealing due to their high complexity and cost.

Electronically controlled diesel fuel injection equipment has been under active development for the past few years. Recent developments in microprocessor technology have created opportunities for better control of fuel delivery and timing than has hitherto been possible. This improved flexibility over the injection parameters offers the possibility of major improvements in diesel engine performance [3]. Improved injection timing flexibility and fast closing times are factors that are known to impact engine emissions [4,5]. However, the improved flexibility also introduces more configuration possibilities, and this complicates the task of selecting optimum injection parameters.

The objective of this research program is to apply advanced modeling techniques to provide guidance for the selection of fuel injection and combustion parameters. This will help in the evolution of more fully optimized, clean and efficient diesel engines. Three-dimensional mathematical models such as the KIVA code are now available and offer a means to help gain the needed understanding of engine combustion and can accelerate the rate of progress in engine development beyond that obtained with traditional 'cut and try' approaches.

In the compression ignition (CI) diesel engine a number of steps are involved in the combustion process. The air is raised to a high temperature on the compression stroke. Multiple high pressure jets of fuel are injected into the chamber which disintegrate into dense vaporizing sprays. After some delay time, self-ignition occurs at points within the sprays. A period of rapid pressure rise follows, during which the vaporized (premixed) portions of the fuel are burned. In the final stages of combustion, diffusion and mixing processes lead to a controlled rate of pressure rise. In some engines, part of the injected fuel impinges on the combustion chamber walls and the final stage of combustion is then influenced by the rate of vaporization of the fuel from the walls. Thus, engine performance (both efficiency and emissions levels) depends on the spatial and temporal details of the atomization of the liquid, vaporization of the droplets, mixing of the fuel and air, and other factors. It is necessary to understand all of these processes and to identify their controlling parameters in order to improve engine performance.

There is evidence that in-cylinder control of pollutant emission levels is possible through the use of ultra-high injection pressures and modified injector nozzle designs or modified in-cylinder gas flow-fields [6,7]. Also, optimized low-heat-rejection (LHR) engines have demonstrated significant reductions in smoke and particulates [8]. Unfortunately, the high in-cylinder gas temperatures of LHR engines also lead to high NOx levels and methods for NOx control such as injection timing retard tend to increase fuel

consumption. It has been difficult to achieve satisfactory pollutant control strategies over wide ranges of engine operation with these approaches alone.

The present advanced modeling techniques will help supply engine and fuel injection design guidelines in this study. The approach taken is to use a three-dimensional code that includes the most advanced available submodels for the important processes that influence diesel combustion. The model accounts for the complex interactions that occur in the turbulent, multiphase, combusting three-dimensional flow in the engine. The complexity of these interactions has made it difficult to gain the necessary level of understanding required for in-cylinder control of emissions by traditional methods.

RESEARCH PROGRAM

The research program was initiated in the Fall of 1989 as a five year program. The emphasis of the research is on the application of a comprehensive engine combustion code to assess the effect of the interacting subprocesses on diesel engine performance, rather than on the development of new models for the subprocesses themselves. The elements of the code are being assembled from existing state-of-the-art submodels. This use of multidimensional modeling as an engine development tool is timely and justifiable due to recent advances in submodel formulations.

The program was expanded to include the modeling of the diesel engine intake process in 1990 due to its importance in the combustion process. A summary of the 1989-1990 research activities has been described in Refs. [12-14]. The research has been organized into three main activities: Part A - Submodel Implementation, Part B - Model Application and Part C - Experiments. Part A tasks are described in the Progress-to-date section (page 7). Part B tasks were started in the the summer of 1991 and are described on page 33. The Part C tasks are described briefly in the Future Work section of this report on page 35.

KIVA CODE

The KIVA code has been chosen for use in the present work since it is the most developed of the available 3-D engine models. The code solves the conservation equations for the transient dynamics of vaporizing fuel sprays interacting with flowing multicomponent gases which are undergoing mixing, ignition, chemical reactions, and heat transfer. The code has the ability to calculate flows in engine cylinders with arbitrary shaped piston geometries, including the effects of turbulence and wall heat transfer. Accuracy of KIVA predictions has been assessed by comparisons with measured cylinder pressures in direct-injection diesel [9], direct-injection stratified-charge rotary engines [10], and in homogeneous-charge reciprocating engines [11].

Due to practical limitations of computer storage and run times it is necessary to introduce submodels into engine codes for processes that occur on time and length scales that are too short to be resolved (e.g., to resolve the flow-field around 10 μm diameter drops in a 10 cm diameter combustion chamber requires about 10^{12} grid points. A practical limit for current computers is about 10^5 grid points). The use of submodels to describe unresolved physical processes introduces some empiricism into the computations. However, the compromise between accuracy and feasibility of computation is justified by the insight which model calculations offer and confidence in the model predictions is gained by comparison with experiments.

In the present work, the KIVA code is being modified to include existing state-of-the-art submodels for important processes occurring in diesel engines. Some of the submodels already appear in the standard KIVA-II code (e.g., the drop drag, turbulence dispersion and turbulence modulation submodels - see Flow Chart of KIVA Subroutines below). Others have already been developed and applied in earlier separate versions of KIVA. Thus, the present research also serves to assemble the most recent models into one comprehensive version of KIVA. The Subroutines that have been modified to data in this effort are identified with asterisks in the flow chart.

PROGRESS TO-DATE

Progress to date in each of the Part A tasks scheduled for the first and second years is discussed in this section and summarized in Table 1 (page 9). Additional details of progress are given in Ref. [14]. Appendix 2 gives additional details of published papers connected with the research activity. Appendix 3 contains FORTRAN source code listings for the spray/wall impingement, combustion and atomization submodels that have been upgraded as part of the research activity.

1. Implement KIVA on TITAN

Due to the high cost of super-computer time, it is important to demonstrate that the KIVA code can be run on dedicated super-workstations. This will ensure that the code is attractive to industrial users. The KIVA-2 code has been running on the Stardent TITAN computer at the Engine Research Center since 9/89. With the model P-3 CPU boards (installed 8/90) we are able to vectorize KIVA-2 satisfactorily. Our benchmark runs indicate that the TITAN now runs only a factor of 10 slower than a CRAY XMP. Also, under ARO funding, the TITAN has been expanded from two to three CPUs, which has increased productivity. In addition, we have been able to secure donations of CRAY computer time from CRAY Research, Inc. and from the San Diego Supercomputer Installation. Thus, the availability of computer time has not impeded progress on the grant.

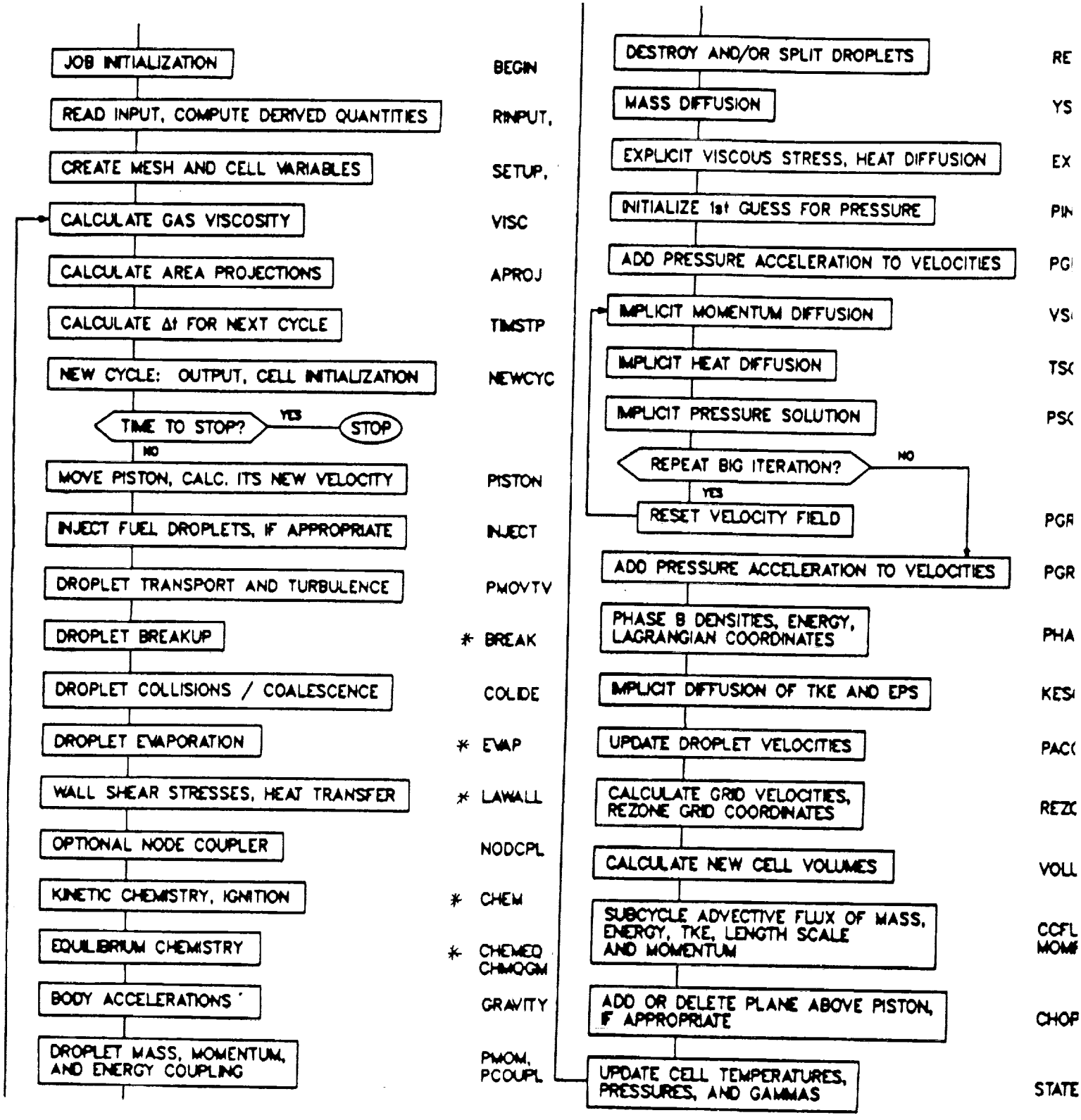

FLOW CHART of KIVA SUBROUTINES Refs. [1,2]
Routines to be upgraded in the present effort are indicated by the asterisks.

A. Submodel Implementation

Table 1 - Submodel Implementation

Phase / Activity		Year 9/1/89 9/1/90 1	9/1/90 9/1/91 2	9/1/91 9/1/92 3	9/1/92 9/1/93 4	9/1/93 9/1/94 5
1	Implement KIVA-2 on TITAN	x	x			
2	Atomization, spray/wall interaction, heat transfer	x				
3	HC and NOx emission	x				
4	Multicomponent fuel Vaporization	x	x			
5	Diesel ignition and combustion		x	x		
6	Soot and radiation			x	x	
7	Intake flow modeling Phase 1 Mesh Phase 2 Mesh Moving valves		x	x	x	

2a. Spray/Wall Interaction

The KIVA-2 code does not contain a spray/wall interaction model and the model of Naber and Reitz [15] has been included in KIVA. This model has been refined further to account for rebounding and sliding drops [16] (see Appendix 3). Upon impact, low Weber number drops rebound from the surface with an angle of rebound that is determined by curve-fitting experimental data on single drops. The need to consider drop rebound was discovered when computations of diesel engine cold-starting were made [16]. In this case, drop rebound provides a mechanism for fuel (vapor) to penetrate back into the central regions of the chamber where the gas temperature is high enough for ignition to occur. Without drop rebound the fuel is predicted to accumulate near the walls where the gas temperature is too low for ignition [16].

2b. Wall Heat Transfer in Premixed-Charge Engine Combustion

Wall heat transfer models have been tested for premixed-charge, spark-ignited-engine combustion as described in Ref [17]. Since the combustion model in KIVA does not account for the influence of turbulence on combustion, a laminar and turbulent combustion submodel has been added for this study (see also task 5 below).

Typical results showing the application of the model to spark-ignited premixed-charge engine combustion are shown in Fig. 1 [17]. As can be seen in Fig. 1a, the computed results (squares) reproduce the form of measured pressure data (circles) very well.

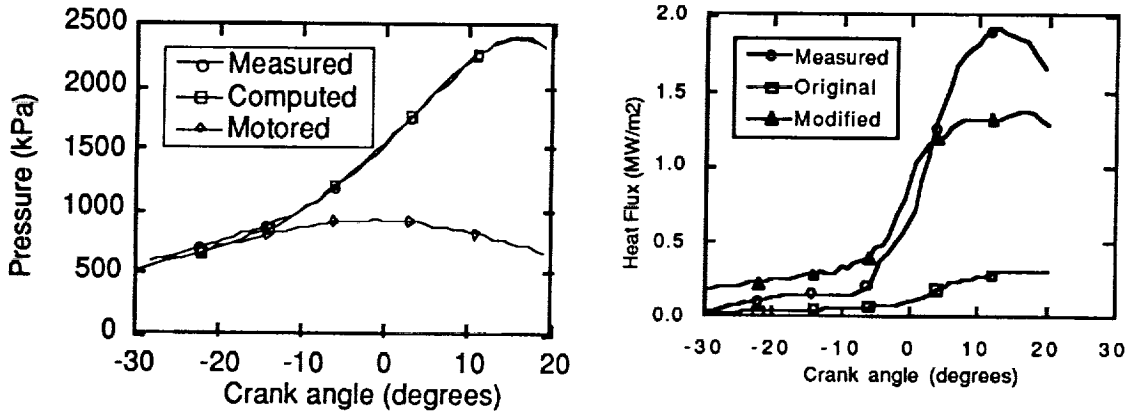

Figure 1 Comparison between measured and predicted cylinder pressure a.) - left, and wall heat flux b.) - right, for premixed-charge engine combustion using the characteristic time combustion model and a heat transfer model that includes the effect of compressibility and unsteadiness (modified case). Engine speed is 1500 rev/min.

The wall heat flux predictions in Fig. 1b were obtained using the original KIVA 'log-law-of-the-wall' heat transfer model (squares) and a modified model that accounts for the effects of compressibility and unsteadiness on the heat transfer (triangles) [17]. The predicted heat transfer is seen to be much improved using the upgraded model, indicating that unsteadiness and compressibility effects need to be considered in engine computations. However it is also evident that additional improvements are needed in heat transfer models, since there is still a 10-20% discrepancy between measured and predicted heat flux values [17]. Reference [17] describes other results that test the wall heat transfer and combustion models over a range of engine operating conditions (motored and fired conditions at two engine speeds).

Further work is in progress on testing the heat transfer models using homogeneous charge, compression ignition engine data (see Task 5, below).

2c. Atomization, vaporization and combustion

Spray computations have been made using our atomization model that is based on considerations of surface wave instabilities [18]. In modeling the atomization process in high pressure sprays, it has been shown that the drop size and penetration length predicted by KIVA are in good agreement with experimental data for non-evaporating sprays at room temperature [18].

However, for high pressure and high temperature sprays, significant discrepancies between the computational and experimental data have been observed [19]. As shown in Fig. 2, using the grid resolution that ensures grid free results in non-vaporizing sprays, the computed vapor penetrations under-estimate the measurements. Since spray penetration directly influences combustion [19], heat transfer, soot formation and other processes, identifying the causes of this discrepancy and making corresponding modifications in KIVA has become essential to continued progress on the grant.

The computations in Fig. 2 were compared with experimental data of Kamimoto et al. [20] for room temperature liquid n-tridecane ($C_{13}H_{28}$) injections from a single hole nozzle (d=0.16mm) into nitrogen gas at 850 - 900 K. The gas pressure was maintained at 3 MPa while the injection pressure were varied from 30 MPa to 110 MPa.

The effects of several factors were considered in the present study, including the influence of vaporization and gas compressibility on the atomization process, and the effects of model constants and numerical parameters.

The spray penetration was found to be very sensitive to the grid size, especially to the grid size near the exit of nozzle, as indicated in Fig. 3. For relatively coarse meshes the penetration increases gradually as the grid size

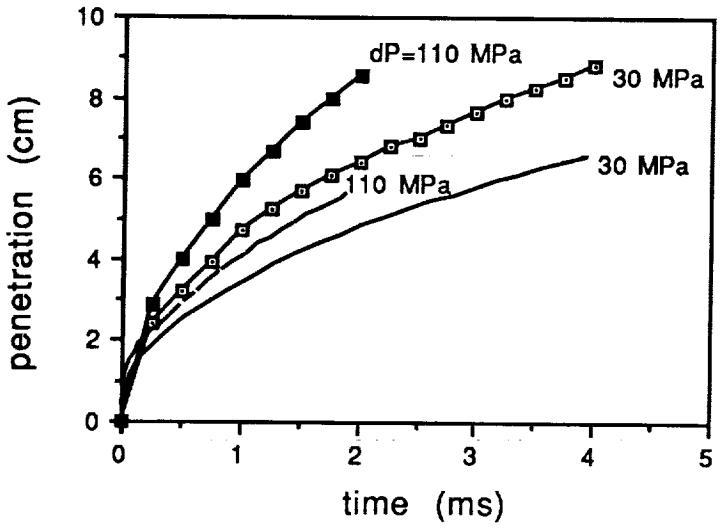

Figure 2 Computed spray vapor penetration versus time. Symbols are measurements of Kamimoto [20] and lines are KIVA predictions (penetration is defined as that distance from the nozzle exit where the fuel vapor concentration reaches 10% of the maximum value in the spray).

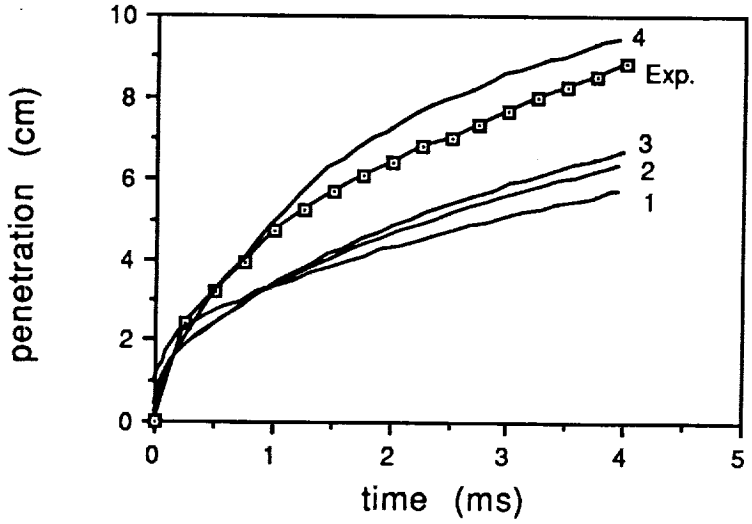

Figure 3 Effect of numerical mesh grid size on spray penetration. ΔP=30 MPa,
Line 1: grid size=1 x 5 mm
Line 2: non-uniform grid 1.25 x 2 mm (near nozzle) to 1.25 x 4.5mm
Line 3: uniform grid 1.25 x 2 mm.
Line 4: non-uniform grid 0.75 x 1 mm (near nozzle) to 0.75 x 3 mm

decreases, which explains why the effect was not noticed in our previous studies [19]. For very fine meshes the penetration is increased dramatically. An explanation for the observed mesh-dependence is that the fuel vaporized from a drop is distributed evenly over the whole computational cell that contains that drop at the end of each timestep in KIVA. This procedure might be reasonable for very fine meshes (or large timesteps) but is hardly satisfied for coarse meshes where the vapor would not have enough time to diffuse or mix over the whole cell. Hence for coarse meshes the local vapor concentration around a drop should be higher than the cell-volume-averaged value. This leads to an over-estimate of the drop evaporation rate and a corresponding under-estimate in the spray penetration.

The implications of this sensitivity to grid resolution for engine computations, where computer cost considerations limit grid sizes, are substantial. One solution to the grid sensitivity problem could be to develop correction procedures for use with coarse grids. For example, assume that instead of occupying the whole cell, the vapor evaporated from a drop is confined within a sphere with radius ~ $(D\ t)^{1/2}$, where D is the vapor diffusivity in the gas and t is the lifetime of the drop. The vapor mass fraction is now averaged over the sphere instead of over the entire cell (until the sphere volume reaches that of the cell, see Fig. 4). Figure 5 shows the penetration thus calculated for a coarse mesh (1.25 x 2 mm) which can be seen to be much improved.

Sub-grid-scale vapor diffusion model

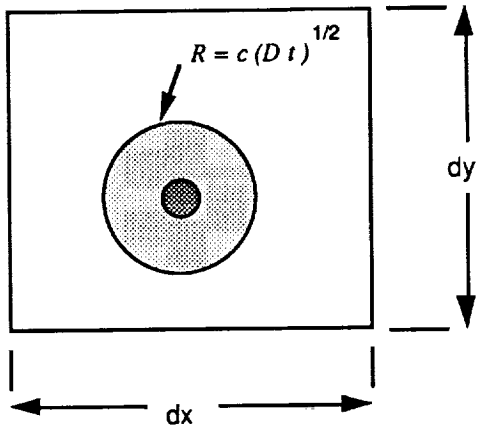

Figure 4 Schematic diagram of the sub-grid-scale vapor diffusion model. The fuel vapor concentration is calculated using the volume of the sphere with radius R instead of the cell volume until the vapor fills the cell.

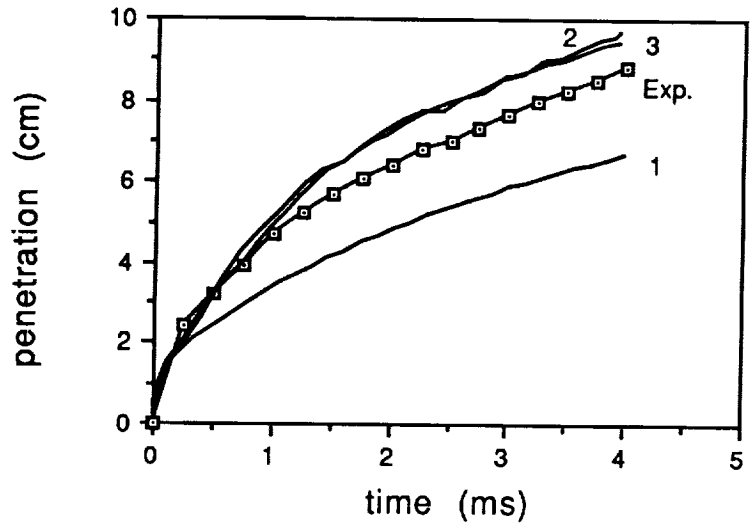

Figure 5 Influence of numerical mesh size on spray penetration.
Symbols: measurements of Kamimoto [20] (ΔP=30 MPa)
Line 1: cell-volume averaged vapor (standard KIVA with - 1.25 x 2 mm mesh)
Line 2 : new vapor-sphere averaged correction method (1.25 x 2 mm mesh)
Line 3 : same as line 1, but with 0.75 x 1 mm mesh.

The comparisons with the constant volume bomb experiments demonstrated the importance of grid resolution in vaporizing spray calculations. For that reason, the engine calculations have been made using fine grids in an attempt to accurately resolve the spray. The computations were made for Cummins NH engine for which extensive experimental data are available with measurements of injection characteristics, cylinder pressure, and flame temperatures from Yan and Borman [21]. Results using a cycle analysis simulation program are available for the same engine [22]. Data, such as the wall temperatures, calculated using the steady state mode were used as input for the initial conditions in the multidimensional calculations as shown in the table below. Additional details of the computations are described in Gonzalez et al. [23].

The calculations were started at inlet valve closing (150 deg BTDC) and considered a 45 degree sector of the engine that included one of the eight spray plumes (i.e., sector symmetry was assumed). The results shown in Figs. 6 and 7 compare spray penetration computations (made without considering combustion) for two different grids. The first grid used 25x6x18 cells with equal spacing in the azimuthal direction. The second grid used the same number of axial cells but had nonuniform azimuthal spacing and gives much increased resolution in the vicinity of the spray - the minimum azimuthal angle is 2 degrees compared to 7.5 degrees in the equally spaced grid. Both grids had 7 axial planes in the bowl and 3 planes in the squish area at TDC. As can be seen, there is a remarkable effect of numerical resolution on the

Cummins Engine Data	
Cylinder Bore	139.7 mm
Stroke	152.4 mm
Compression ratio	13.23
Displacement	2.33 liters
Number of spray nozzle orifices	8
Nozzle hole diameter	0.2 mm
Spray axis, angle from head	18º
Combustion chamber	Quiescent
Piston crown	Mexican hat type
Engine speed	1500 r/min (constant)
Overall equivalence ratio	0.6
Air flow rate	0.353e-2 kg/cycle
Fuel flow rate	0.144e-3 kg/cycle
Intake tank pressure	148.2 kPa
Intake tank temperature	302 K
Engine temperatures at IVC	(constant during the cycle)
Cylinder wall	405 K
Cylinder head	486 K
Piston surface	578 K
Valves face	773 K
Mass average gas temperature at IVC	359 K
Cylinder pressure at IVC	157.9 kPa
Swirl number	1.0
Fuel	Tetradecane
Injection starts	18º btdc
Injection ends	11º atdc

predicted spray penetration at TDC. It should be noted that these computations were made using the atomization model of Reitz [18] with no modification to the vaporization routines.

Figure 8 shows computations that include the effect of combustion, made using the same grids as those for the results in Figs. 6 and 7. As can be seen, the fine grid computation gives a higher predicted peak cylinder pressure than the coarse grid computation. However, the predicted pressures still underpredict the measured pressures substantially. The results shown in Fig. 9 demonstrate that the details of the combustion model have a large effect on the predicted cylinder pressures, particularly for the fine grid computations. For Fig. 9 the computations used a reduced value of the pre-exponential constant, viz. $K_1 = 7.68 \times 10^8$. This value of K_1 was found to give the highest possible peak cylinder pressure for both the fine and the coarse grid cases. Further reductions in K_1 caused unrealistically long ignition delays. It is seen that the discrepancy between measurements and predicted cylinder pressures is reduced significantly for the fine grid computation with the revised combustion model constant.

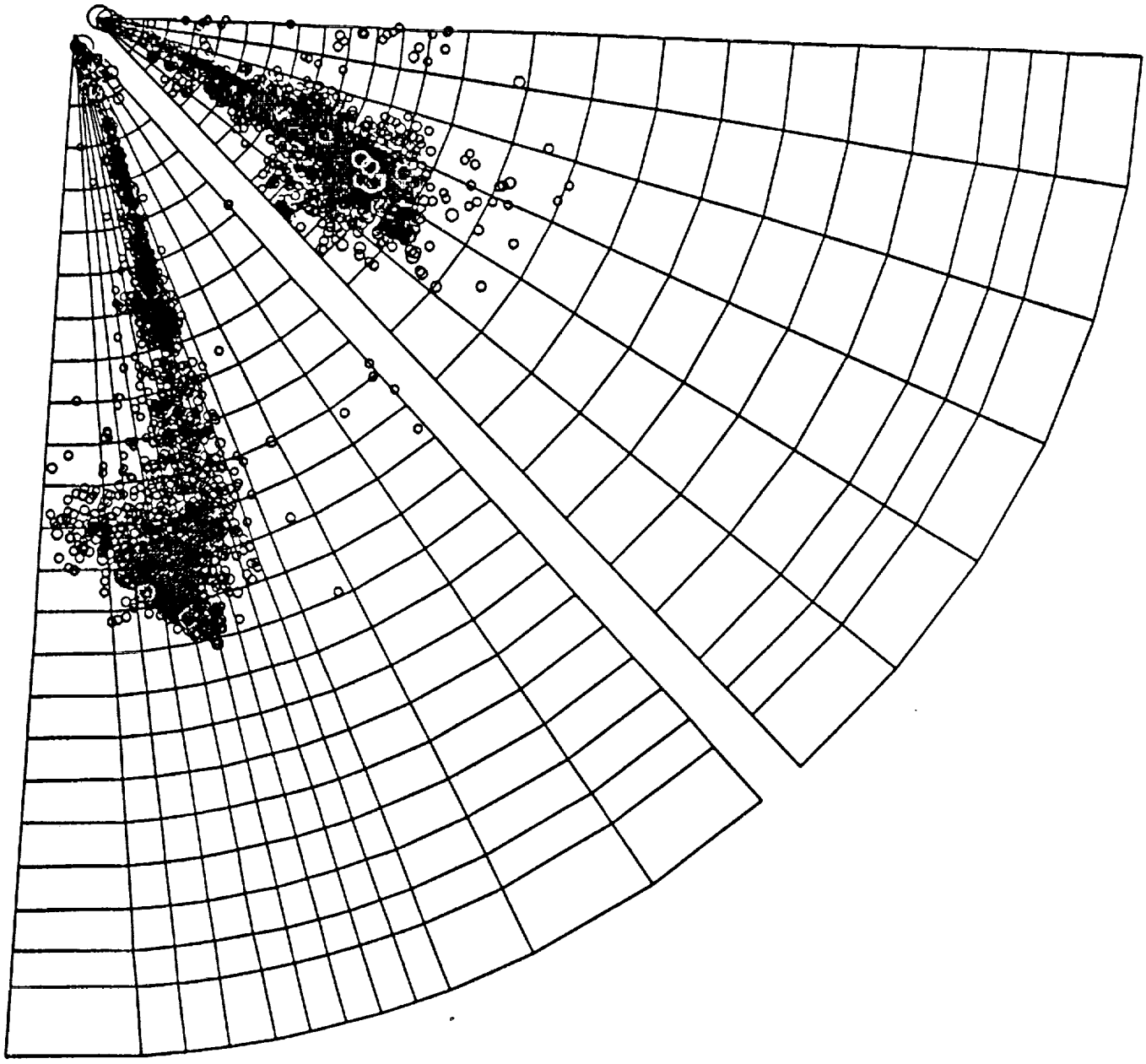

Figure 6 Plan view of sprays showing effect of grid resolution on predicted spray penetration. TDC, 1500 rev/min, computations made without considering combustion. Top: Coarse grid which uses 25x6x18 cells. Bottom: Fine grid which uses 24x12x18 cells with non-uniform azimuthal spacing.

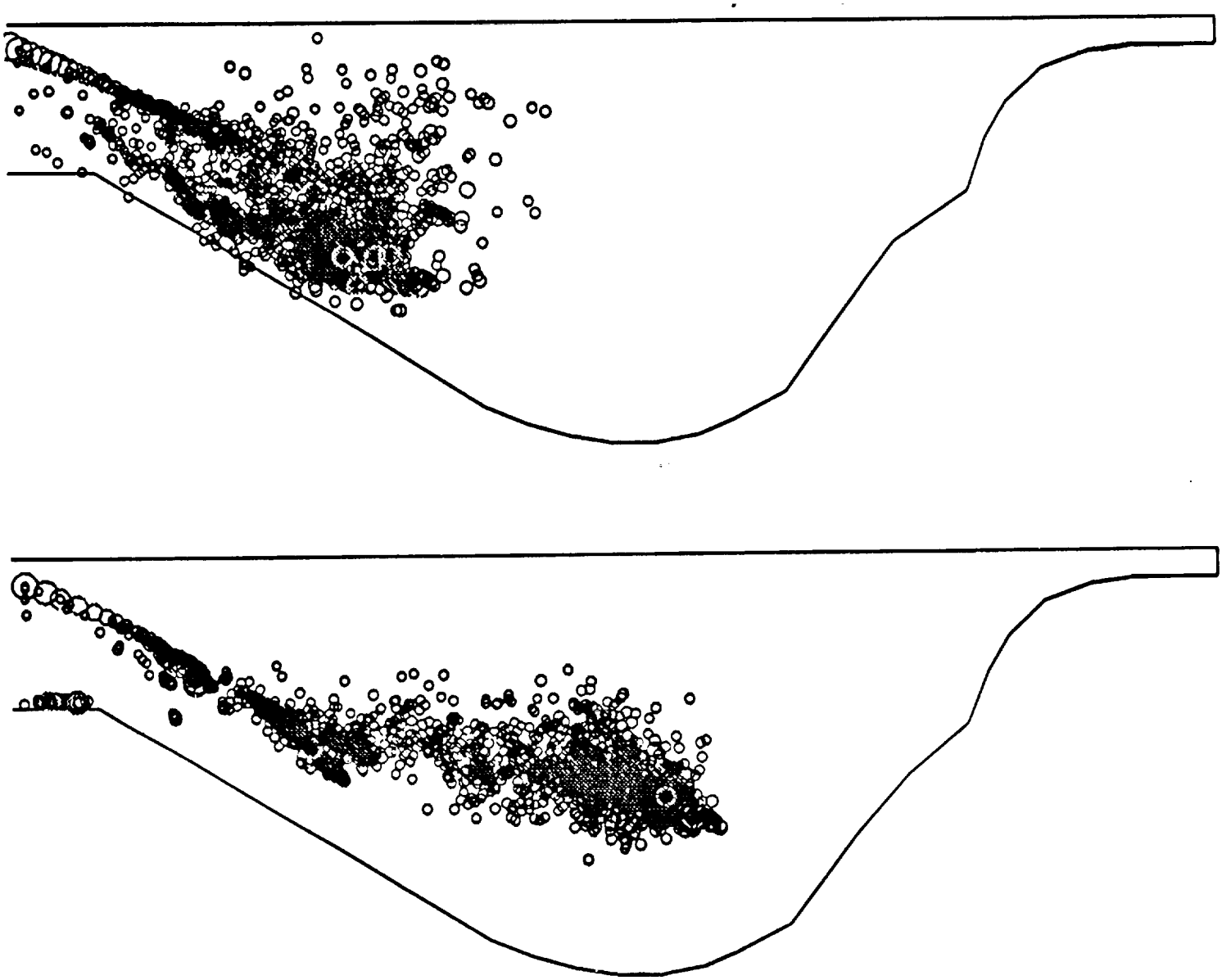

Figure 7 Elevation view showing effect of grid resolution on predicted spray penetration for the conditions of Fig. 17. Top: Coarse grid which uses 25x6x18 cells. Bottom: Fine grid which uses 24x12x18 cells with non-uniform azimuthal spacing.

The reason for the improved pressure predictions is seen in Fig. 10. Figure 10 shows the predicted temperature contours and spray drop locations in the chamber at TDC in a plane through the center of the spray for the coarse and fine grid cases of Figs. 6, 7 and 9 (i.e., using the revised combustion model constant K_1). As can be seen in the fine grid results, the high temperature contours are now located closer to the edge of the bowl, in better agreement with the experimental observations of Yan and Borman [21] who, using a radiation probe mounted in the cylinder head, found that the flame reached the piston bowl outer surface between 6 deg BTDC and 1 deg ATDC. However, the coarse grid temperature contours show that the flame is still confined to the region near the nozzle. (The position of the high temperature regions in the combustion cases of Fig. 10 is seen to be correlated with the spray penetrations (without combustion) shown in Fig. 7.)

The sensitivity of the fine grid results to the combustion model constants indicates that further optimization of the results in Fig. 9 will require improved combustion models. For example, the simplified Arrhenius-type combustion model used in this study does not specifically account for ignition processes nor does it include the effect of turbulent mixing that is known to be important in diesel combustion. This is the subject of Task 5 below.

The atomization model itself has been improved by extending the stability analysis to consider an evaporating liquid surface. In this analysis [24] the evaporation flux of a perturbed surface with local curvature R was assumed to be proportional to that of a spherical droplet of radius R, and the kinematic condition (jump condition) at the liquid-gas interface is modified to include the effect of surface evaporation velocity. The recoil force due to evaporation is also taken into account in the interface normal stress equation [25,26].

A new dispersion equation was obtained as shown in Fig. 11, where Va is a dimensionless parameter representing the evaporation level. Figure 11 shows that surface evaporation reduces both the growth rate and wavenumber of the most unstable waves; hence the surfaces waves break slower and produce larger droplets. The influence of this phenomenon on the atomization process is being evaluated.

An additional consideration is the influence of the compressibility of the ambient gas on the atomization process. In the stability analysis of Reitz [18], it was assumed that both liquid and gas are incompressible. The validity of this assumption is questionable for the high injection pressures of interest in diesel engines since the Mach number often exceeds 0.3. To study the gas compressibility on high speed spray, we have adopted a method where the dynamic pressure in the gas includes the effect of Mach number following Bradley [27,28]. The effect of gas compressibility on atomization is being assessed.

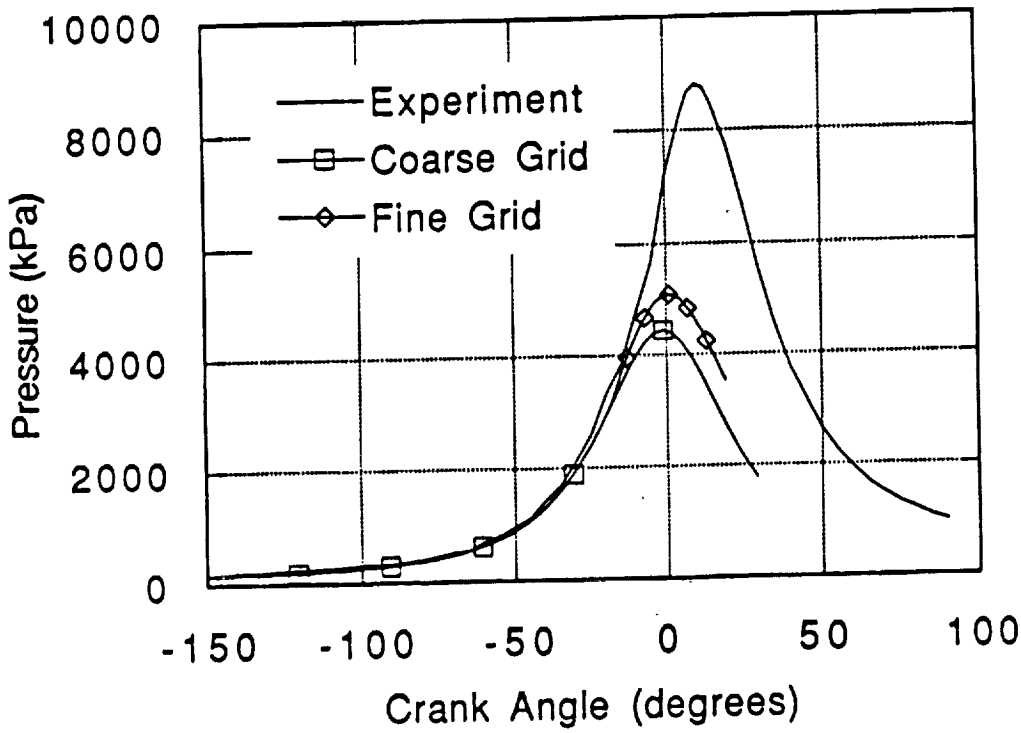

Figure 8 Predicted cylinder pressure using the unmodified combustion model with $K_1 = 3.68 \times 10^{10}$ showing effect of grid resolution for the coarse and fine grids of Fig. 6.

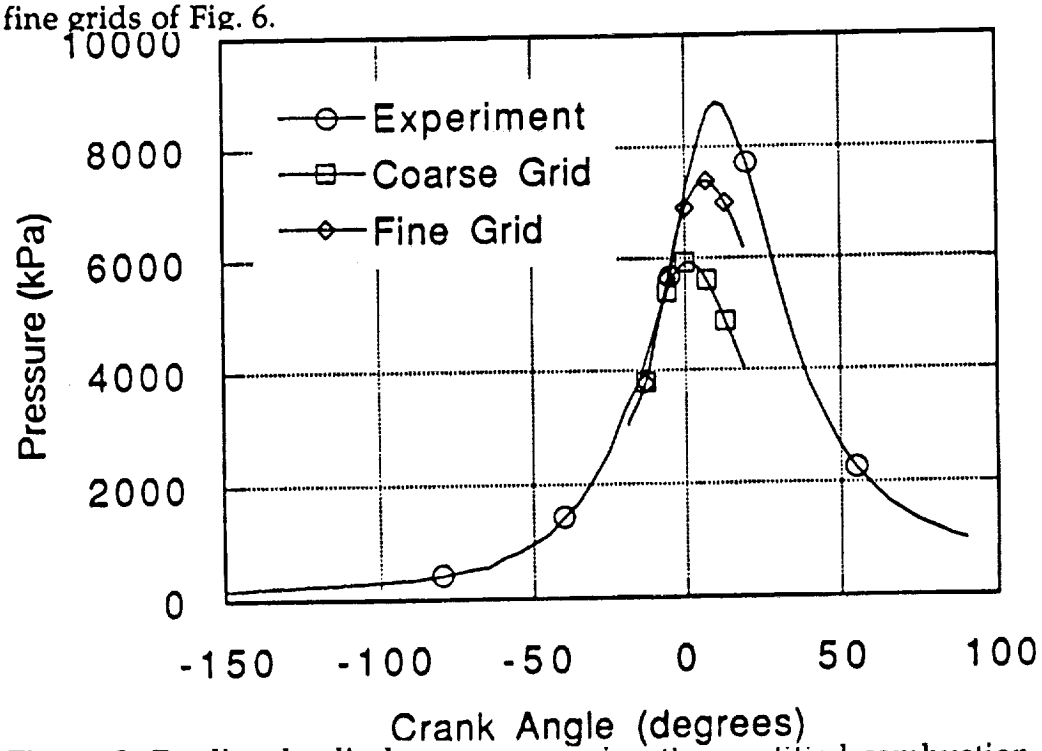

Figure 9 Predicted cylinder pressure using the modified combustion model with $K_1 = 7.68 \times 10^{8}$ showing effect of grid resolution for the coarse and fine grids of Fig. 6.

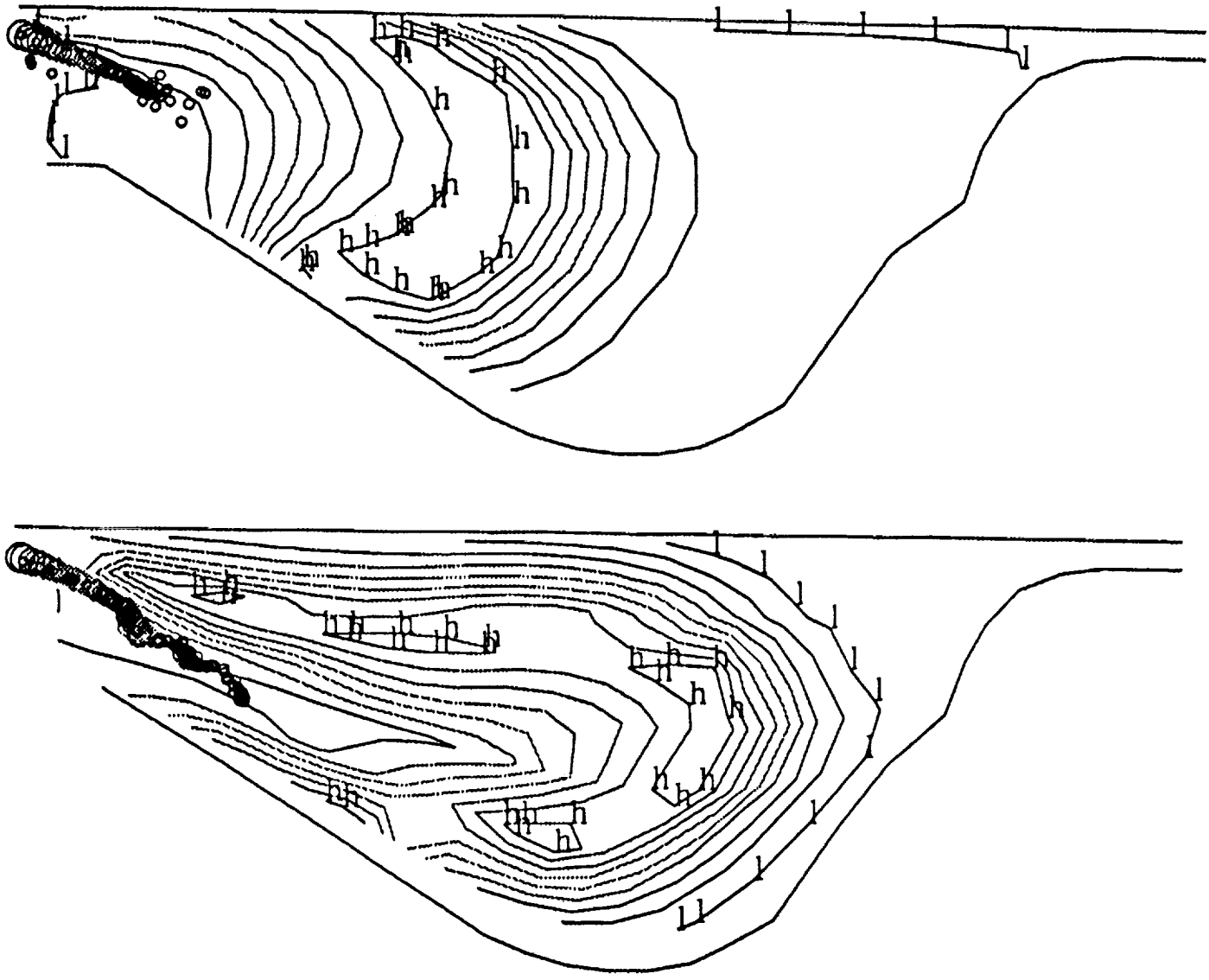

Figure 10 Elevation view showing effect of grid resolution on predicted spray penetration and temperature contours for the conditions of Fig. 6. Top: Coarse grid which uses 25x6x18 cells (h=2660 K, l=917 K). Bottom: Fine grid which uses 24x12x18 cells with non-uniform azimuthal spacing (h=2720 K, l=1090 K).

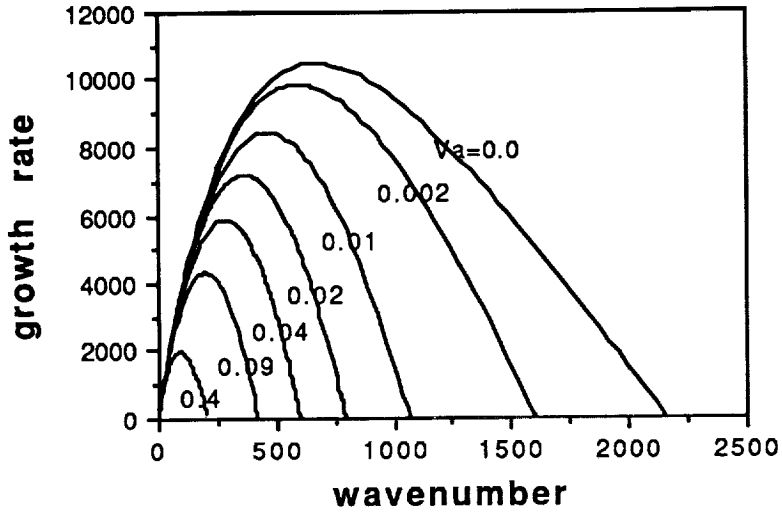

Figure 11 Predicted wave growth rate versus wavenumber for different evaporation levels from the modified dispersion relationship.

3. HC and NOx emission

The combustion model specifies the rate of conversion from reactants to products using a characteristic time which is controlled by the longer of the local turbulent mixing or laminar kinetics times and is formulated such that correct thermodynamic equilibrium is recovered in the burned gas [17]. The correct burned-gas temperature is needed for accurate NOx predictions using the Zeldo'vich kinetics model which has been included in KIVA . The combustion and NOx models are included in Subroutine Chmprn in Appendix 3.

The combustion model automatically predicts unburned hydrocarbon (HC) in regions of low gas temperature or high equivalence ratio where the characteristic chemistry time is large and the conversion of fuel to products is arrested. Unburned HC and NOx predictions will be examined in the model application project (see Table 2, page 33).

4. Multicomponent Fuel Vaporization

Our initial attempts to model diesel engine combustion phenomena revealed major qualitative discrepancies between computations and experiments [19] (see also Task 2 above). These discrepancies motivated a critical evaluation of single component drop vaporization models.

The fuel considered in the study was hexadecane (T_{cr}=725 K), and a single 50-μm diameter droplet was injected at a velocity of 100 m/s into a cylinder

containing air at 40 atm and 800 K. The mesh used in this phase had 20x1x60 cells (1 x 2 mm cells).

The original KIVA vaporization model is a low pressure model that is based on the following assumptions : a. spherical symmetry, b. single component fuel, c. uniform drop temperature, d. constant fuel density and, e. unity Lewis number. Assumptions d. and e. have been removed in the present effort, and the details are summarized below. The preparatory phases of modeling multi-component fuels (assumptions b. and c.) has been completed. The spherical symmetry assumption was considered to be reasonable for stable, non-breaking drops.

Since the injected drops undergo a significant temperature variation during their life-time and the properties of the fuel change considerably, the governing equations for vaporizing drops were rewritten to include variable liquid density which was not accounted for in the original KIVA.

Figure 12 shows the predicted drop size variation (drop radius non-dimensionalized by initial radius) as a function of time using the original KIVA vaporization model, and using the new model that accounts for variable liquid density. With variable density, the drop size increases in the heat-up period. This size increase is accompanied by an increase in the available surface area which increases the vaporization rate resulting in a shorter drop lifetime.

An additional factor that was considered is the influence of mass transfer on the heat transfer for vaporizing drops. Various corrections have been proposed in the literature but the one used in KIVA assumes that the Lewis number of the fuel vapor is unity. Computational results under the conditions of interest show that the Lewis number is typically between 4 and 5. This observation has motivated the use of the correction of Priem et al. [29] in place of the KIVA correction.

As can be seen in Fig. 12, the variable Lewis number effect (which represents superheating of the vapor around the drop) also leads to shorter drop lifetimes. The modified version of KIVA now includes both variable fuel density and Lewis number effects, and the results are seen in Fig. 12 to lead to a significant reduction in the predicted drop lifetime. Other results show that these reductions in lifetime are not as large at lower values of the drop-gas relative velocity, as would be expected from the form of the correction terms.

Work is also in progress on implementing a multi-component fuel vaporization model into KIVA that is based on the works of Refs. [30,31]. Preliminary results are shown in Fig. 13 for a 50 μm diameter, 50% pentane/50% octane drop at 300 K injected into a 800K, 4 MPa nitrogen environment. The drop was injected at 100 m/s.

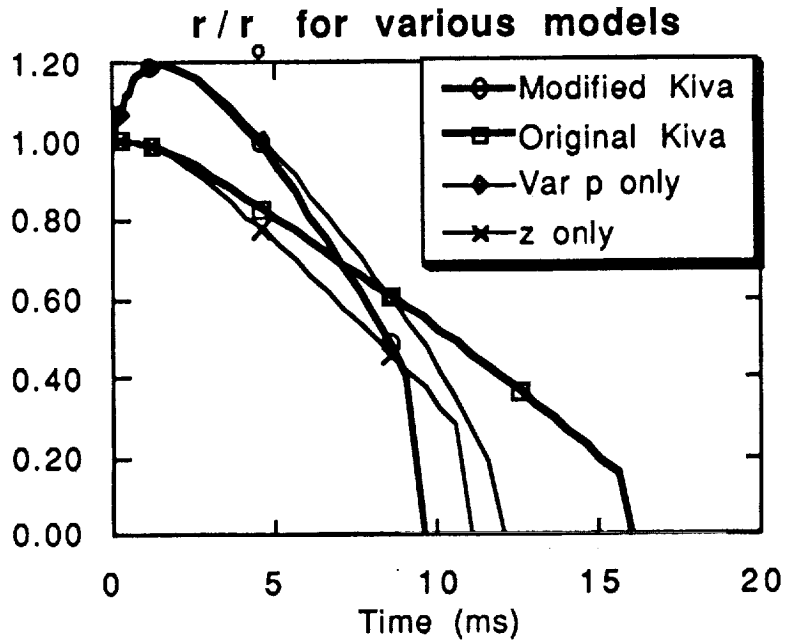

Figure 12 Predicted drop size variation with time showing the effect of variable fuel density (var p) and non-unity Lewis number (z only). Modified KIVA results includes both density and Lewis number effects.

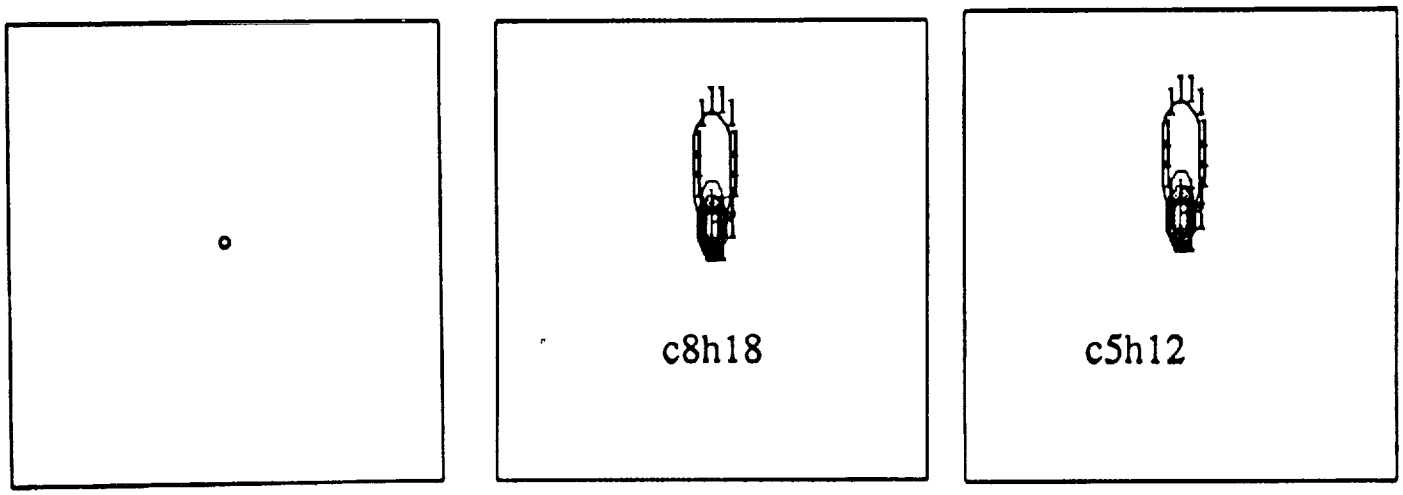

Figure 13 Predicted fuel drop location and concentration contours at 2 ms after injection (the injector is located at the top center of the diagrams). 50 μm diameter, 50% pentane/50% octane drop at 300 K injected into a 800K, 4 MPa nitrogen environment. Chamber is 40 mm in diameter.

5. Diesel ignition and combustion

Our preliminary modeling of diesel ignition and combustion used kinetic constants from the ignition study of Bergeron and Hallet [32] to specify the Arrhenius rates for the laminar chemistry time in the combustion model [19,23]. In the current effort, the laminar and turbulent characteristic time combustion model of Abraham et al. [33] that was used for the spark-ignited engine studies (see Task 2, above) has been extended to allow predictions of ignition [34].

The homogeneous charge, compression-ignition engine experiments of Boggs [35] were used for this study. These experiments were performed in the CFR engine at the Center using ethylene fuel. Six cases were studied that include two engine speeds (600 and 1200 rev/min), two swirl ratios (1.2 and 8) and two compression ratios (10.5 and 6.3 - equivalence ratios of 0.24 and 0.4). Details of the engine geometry are given below. The residual amounts and exhaust temperature were estimated by using the method of Yuh and Mirsky [36].

CFR Engine specifications

cycle	4-Stroke
Bore	83.1 mm
Stroke	114.3 mm
Connecting Rod Length	254.0 mm
Displacement	620 c.c.
Valve	Supercharge cam
Lift	7.93 mm
Intake timing	Open 15 ^{0} BTC, Close 50 ^{0} ABC
Exhaust timing	Open 50 ^{0} BBC, Close 15 ^{0} ATC
Cooling System	Evaporative, atmospheric pressure Water coolant

The time rate of change of the partial density of species i , due to conversion from one chemical species to another, is given by $dY_i/dt = -(Y_i - Y_i^*)/ t_c$ [33], where Y_i is the mass fraction of species i , and the * indicates local and instantaneous thermodynamic equilibrium values. t_c is the characteristic time for reaction which is assumed to be the sum of the laminar (high temperature) chemistry time t_ℓ , the turbulence mixing time t_t , and ignition (low temperature) chemistry time t_i, which was not present in the original combustion model, i.e., $t_c = t_\ell + t_t + t_i$.

The ignition characteristic time t_i was modeled using data from elementary initiation reactions of ethylene [37] and has the Arrhenius form. Since this

timescale represents many possible reaction paths, it was felt justifiable to adjust the pre-exponential constant slightly to give the best overall agreement with the experiments. It was found to be possible to match all cases reasonably well with one set of ignition model constants. Crevice flow effects were found to be significant for this engine, and the crevice flow model of Reitz and Kuo [38] was implemented in KIVA. It was necessary to measure the piston-cylinder-liner crevice volumes on the engine.

Typical results showing comparisons between measured and predicted cylinder pressures are given in Fig. 14. The level of agreement is quite good. It should be noted that this level of agreement was not possible if the turbulent mixing timescale was not included as a parameter in the combustion model.

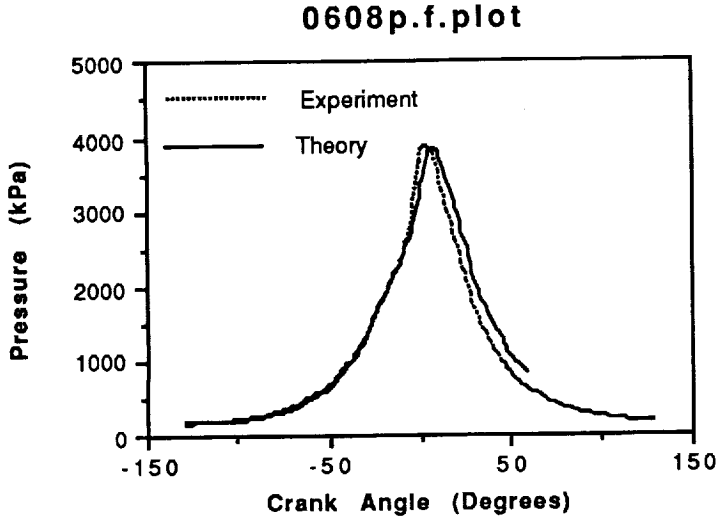

Figure 14 Comparison between computed and measured cylinder pressures for compression ignited, homogeneous charge engine combustion (engine speed 1200 rev/min, compression ratio 11.5, swirl ratio 8.0, equivalence ratio 0.24).

This important conclusion implies that thermal mixing phenomena control the rate of combustion, even in this engine that is characterized by the absence of a propagating flame. The characteristic timescales are shown in Fig. 15. As can be seen, ignition is controlled at low temperatures by the ignition timescale. Notice that the high temperature laminar chemistry timescale never plays a role in determining the combustion rate since it is always smaller than the other characteristic times.

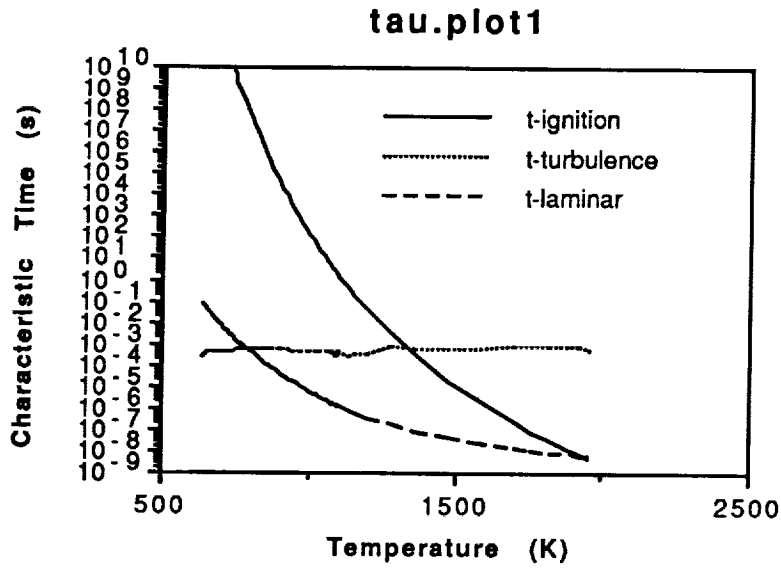

Figure 15 Characteristic combustion times versus cylinder gas temperature for the compression-ignited, homogeneous-charge engine case of Fig. 14.

The location of the combustion regime for this engine has been compared with the internal combustion engine regimes proposed by Abraham et al. [39] which consider the Damkohler number (ratio of turbulence mixing time to the reaction time) and the turbulent Reynolds number (based on the integral length scale). The present engine combustion was found to be located in the distributed reaction regime once combustion starts.

The corresponding wall heat flux predictions are compared with the experimentally measured values in Fig. 16. The phasing of the heat flux is well predicted, although the peak values are under-estimated by amounts that are similar to those for the spark-ignited engine shown in Fig. 1. The implication of these results about the necessity to include the effect of combustion in wall heat transfer models is being investigated.

The next phase of the work will involve the above characteristic time ignition model, and other ignition models to improve spray combustion predictions (see Task 2 above).

6. Soot and Radiation

Work will begin on this effort in the next year (see Future Work).

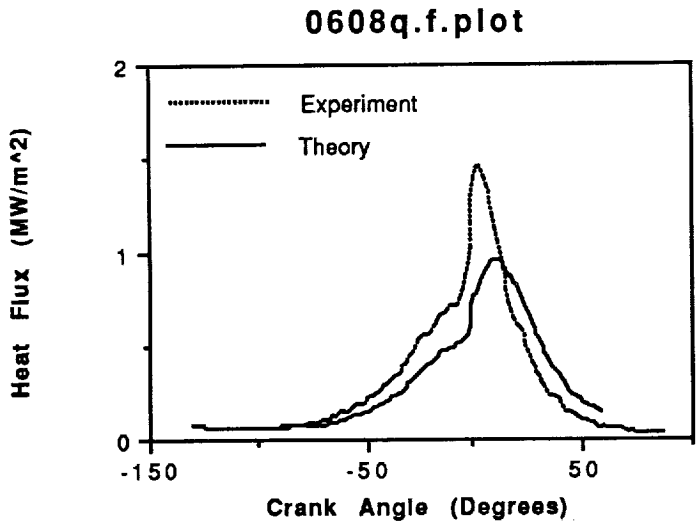

Figure 16 Comparison between predicted and measured wall heat flux for compression ignited, homogeneous charge engine combustion (engine speed 1200 rev/min, compression ratio 11.5, swirl ratio 8.0, equivalence ratio 0.24).

7. Intake Flow Modeling

The intake flow work is proceeding on schedule. Initial phase one calculations are successfully being performed to evaluate simple flow fields and different grid schemes. In addition, grid generation for realistic multi-valve port geometries is nearing completion.

Intake flow modeling is being implemented using KIVA-3. This is a new, unreleased version of KIVA for which the Engine Research Center is serving as a beta test site. The major advancement of KIVA-3 over previous versions is the use of unstructured grids. This provides an efficient means of representing complex, multi-domain geometries such as the intake port, valve, and cylinder. In addition, KIVA-3 retains the ability to model moving grids and allows different regions to become disconnected during a calculation.

KIVA-3 is now tested and running on the Cray machines used at the ERC. An interface between KIVA-3 and the graphical post-processing program, PLOT3D, has also been implemented. Initial calculations on simple (but multi-domain) geometries are being carried out to test feasibility of gridding schemes and for initial examination of intake flow fields.

An example calculation is shown in Fig. 17. The initial gridding and sample calculation used a stationary valve head and stem with a moving piston and considered the intake stroke. The 3-D view of the velocity field in Fig. 17 was obtained by converting KIVA-3's post-processor to give PLOT3D compatible

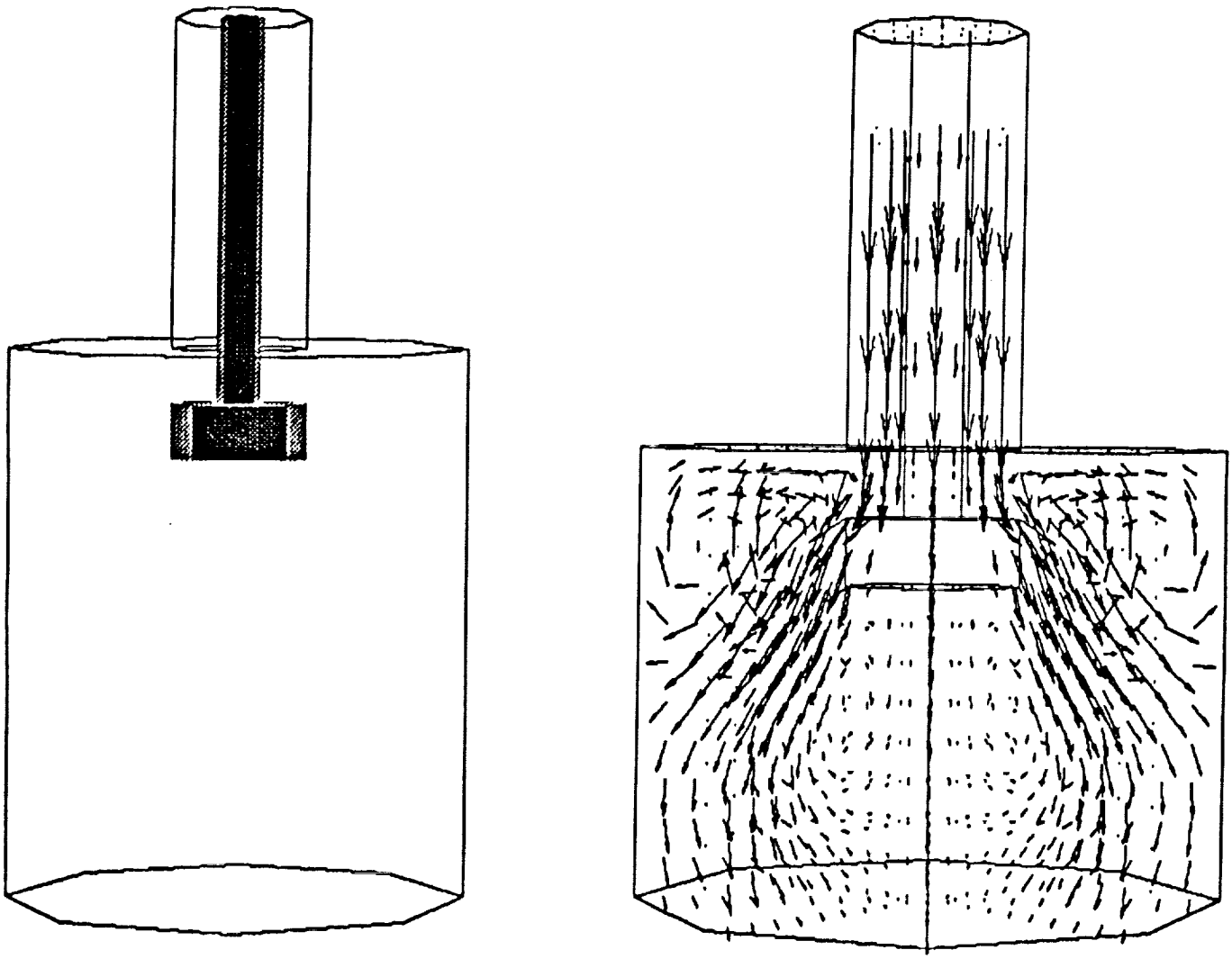

Figure 17 Intake flow computation using KIVA-3 for a centrally located stationary valve at 120 degrees after top-dead-center.

output. The computational grid was created using the KIVA-3's pre-processor. A constant pressure boundary condition was used at the top of the intake port. The flow enters the cylinder and is deflected radially outward by the valve head. The cylinder wall deflects the flow downwards and a large scale recirculation pattern is established. Despite the coarse grid used in these initial computations, the flow patterns are very similar to visualization experiments by Eaton and Reynolds [40] in a motored engine with a centrally located valve.

Grid generation remains a major task for the intake flow calculations, since it is so time consuming to create a complex 3D grid. Work is underway to replace KIVA-3's simple grid generator with the GRIDGEN code developed by General Dynamics under Air Force contracts. This code has been selected over the EAGLE code because it is more flexible and it makes use of our Silicon Graphics IRIS workstation. Also, GRIDGEN is being used by many other users (we have joined a grid generation users group (NAS SigGrid, NASA Ames)).

Grid generation with GRIDGEN is a three step process. The first step is the division of the geometry into logical blocks. The second step is the formation of a computational grid on each face of each block. This establishes the surface grid that will be used to generate the volume grid in the third step. The final step is the generation of the 3D volume grid. This is a fairly intensive calculation that is currently implemented only on CRAY computers running COS. Modifications to run under UNICOS or on the Stardent Titan are currently being investigated. Results of this step are transferred back to the Iris for visualization. The file containing the 3D grid information is then reformatted for input to KIVA-3.

The basic geometry used in step one of this process is obtained from digitized data of the intake manifold. An expanding flexible foam was used to transform the manifold's internal features into a mold form. Liquid acrylic was poured around the foam form to create a full size replica of the original manifold geometry. The acrylic casting was then cut into slices. Features machined into the acrylic block (see Fig. 18) allow the longitudinal position of each slice to be determined.

A computerized video measurement technique transposes the physical geometry contained in the cross sections into coordinate data. This technique digitizes the images using edge finding algorithms, and calculates the line coordinates using parametric splines. The output is the three dimensional coordinates that correspond to the cross section geometry. The technique is repeated for each slice until all geometry is recorded. Finally, the cross section geometry is combined and formatted to serve as input for step 1 of the grid generation process.

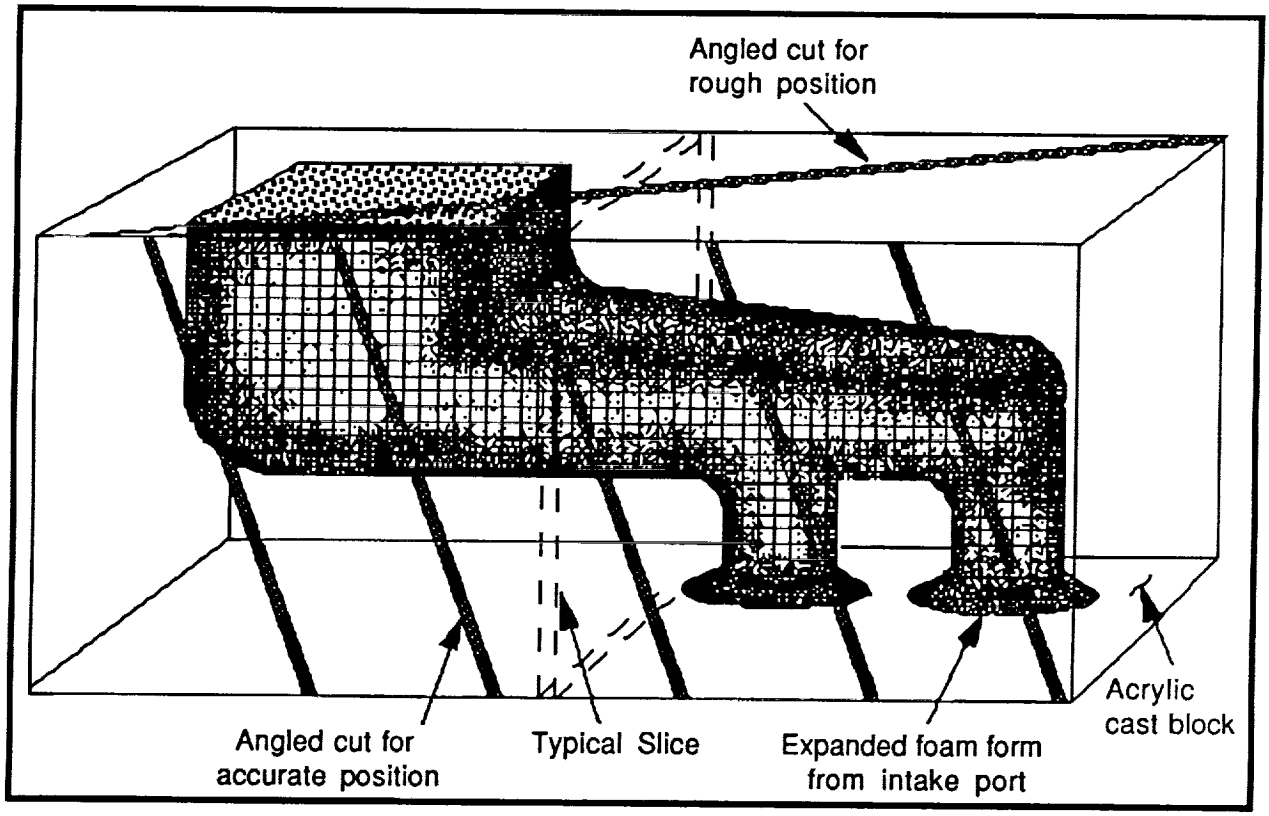

Figure 18 Schematic showing foam mold of intake port and acrylic block used to obtain digitized geometry.

Figure 19 shows a grid of a Caterpillar engine intake port (the interior grid is removed for clarity) that has been generated using this method.

Various approaches for implementing a moving valve into KIVA-3 are currently being evaluated. The moving valve requires that different regions of the grid move relative to each other. This will implemented with a variation of the "snapper" algorithm used to move the piston in KIVA-3. This algorithm maintains grid point connectivity by snapping grid points between neighboring cells as the grid moves. The snap occurs when the gird has moved a specified percentage of a cell distance. A method of using the snapper algorithm with the moving valve has been developed and is shown schematically in Fig. 20. Figures 20 (a) and (b) show the grid as valve begins to move upwards; all vertices are active in the calculation until the grid reaches a deformation limit. At the deformation limit (Fig. 20 (c)), the snapper algorithm inactivates the six open circle vertices and moves the eight square vertices down to the valve surface. The six vertices on the valve face are moved down into the cylinder region and replaced by new vertices. Volume weighted interpolation is used to reassign all properties associated with snapped vertices and their cells.

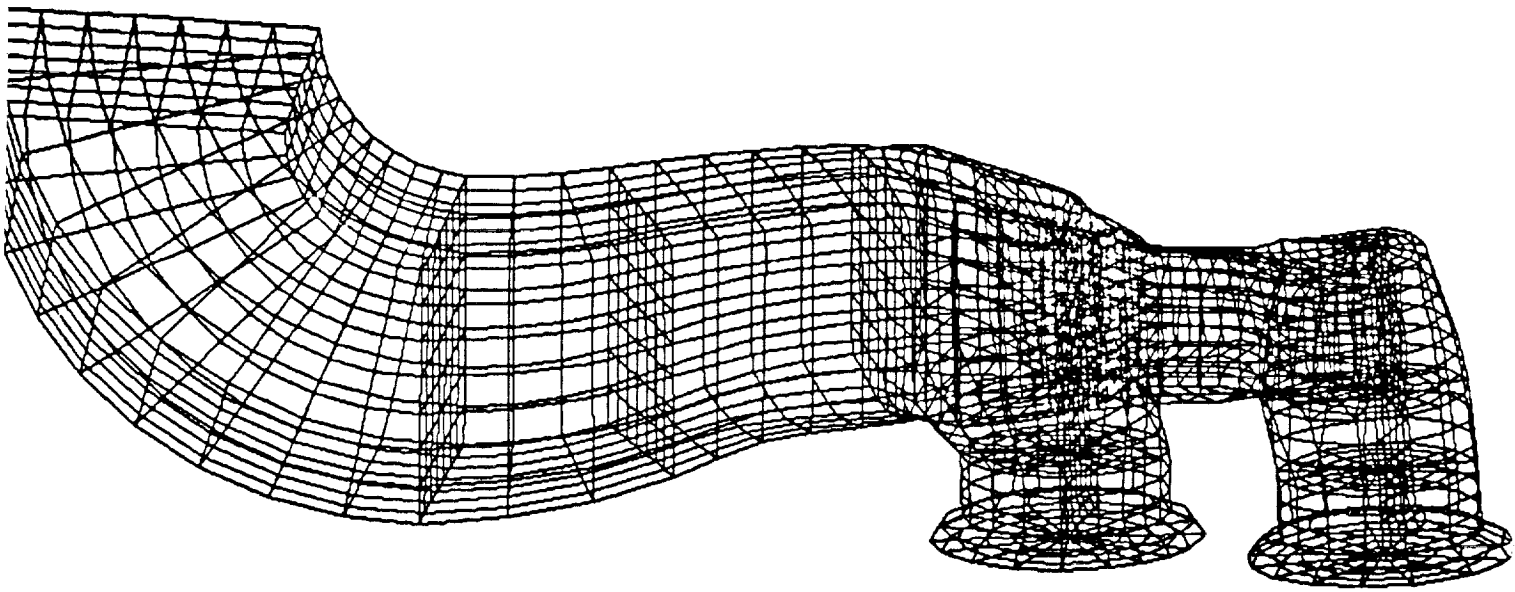

Figure 19 Grid generation for a single cylinder Caterpillar engine intake port.

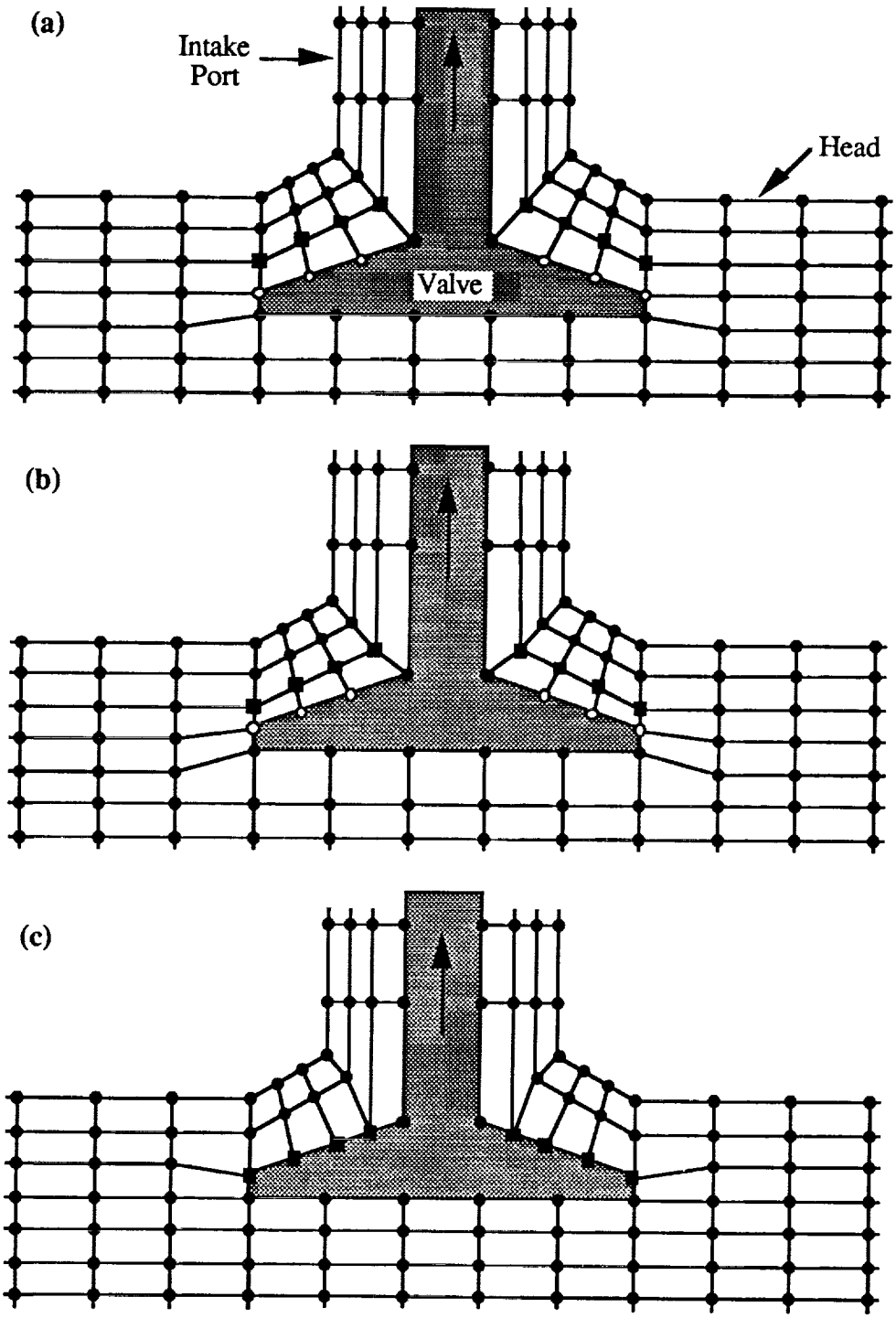

Figure 20 Schematic showing use of "snapper" algorithm for moving valve. Open circles and squares are used to show the movement of vertices as the valve closes.

B. Model Application

The model application tasks in Phase B are presented in Table 2. The individual projects are discussed below in the Future Work section.

Table 2 - Model Application

Topic	/ Study	Year 9/1/89 9/1/90 1	9/1/90 9/1/91 2	9/1/91 9/1/92 3	9/1/92 9/1/93 4	9/1/93 9/1/94 5
1	Ignition delay		x	x	x	
2	Fuel-air mixing			x	x	x
3	Wall impingement			x	x	x

FUTURE WORK

The proposed work schedule for the period 6/91 - 9/92 for Parts A (Model Implementation) and B (Model Application) can be seen in Tables 1 and 2. The plan of work for Part C (Engine Experiments) is discussed on page 35. Details of some of the individual tasks are described below.

Part A - Multi-component fuel vaporization and atomization

We will continue to study the influence of vaporization on atomization [24] and assess the effect on diesel combustion modeling. In addition we will extend our implementation of the multi-component fuel vaporization model in KIVA. To save computer time and storage, we are exploring methods where the droplet internal temperature and concentration fields can be solved using at most ten internal grid points per drop. As the drop vaporizes, the number of internal grid points is reduced and eventually, when the drop size becomes sufficiently small, the lumped parameter approach of KIVA is recovered.

Part A - Diesel Ignition

We will extend our ignition model to consider spray ignition. In this case the high temperature constant volume bomb experiments of Kamimoto [20] will be used as a starting point, since they also include cases with combustion. Our

previous diesel combustion computations [19,23] that modeled the data of Yan and Borman [21] for a Cummins NH engine will be continued. We will also be making use of measured pressure data from the Caterpillar engine experiments (see Part C). As part of the ignition modeling effort, we will explore the use of the Theobald ignition model [41].

Part A - Soot and Radiation

Soot model development will start by considering the soot model proposed by Gentry et al. [42] for coal slurry applications which will be implemented. Due to the complexity of the soot formation and destruction processes, it is anticipated that soot concentration predictions will be qualitative only. It is planned that the radiation model of Chang and Rhee [43] will be adapted for use in this study. This model assumes the Rayleigh-limit for the soot emissivity and a band model for the gas emissivity. More complicated radiation models that require solution of the radiation transport equation and that account for scattering by the spray drops are available [44]. However, in view of the uncertainties about soot concentrations, this additional complexity is not considered to be warranted at the present time. Much work is being done in this area and it will be monitored for its appropriateness for inclusion in KIVA.

Part A - Intake flow modeling

We expect to be able to perform computations for realistic intake port and valve geometries in the near future. Comparisons will be made to steady state flow bench experimental data. Swirl measurements and flow visualizations will be made for comparison to the KIVA calculations using the Caterpillar multi-valve intake port. Any discrepancies between experiments and calculations will be investigated. This may require improvements to the turbulence model in KIVA so that the high shear through the valve curtain is more accurately modeled.

Part B - Ignition delay

Computations of the influence of diesel ignition delay on emissions will be made. The data of Yan and Borman [21] will be used to verify the accuracy of the model. The goal is to explore research issues such as the influence of the injection timing and the number of injector holes on ignition delay. Over-mixed vaporized fuel is thought to be responsible for the increase in HC emissions found with an increased ignition delay. The influence of the fuel injection parameters on multi-component fuel vaporization and mixing during the ignition delay and the early stages of the diffusion burning phase will be studied in later phases of the project.

Part B - Fuel-air mixing, Spray/wall impingement

Computations of fuel-air mixing and spray wall impingement will begin in the summer of 1992. The location and extent of over- and under-mixed fuel-air regions within the combustion chamber influence engine operation and emissions. Particulates are thought to be formed when under-mixed regions are exposed to high temperatures. The influence of the fuel injection parameters and in-cylinder flow details on mixing and combustion during the diffusion burning phase will be assessed.

The effect of wall impingement on in-cylinder fuel-air distributions and combustion will also be considered. In particular, differences between sprays whose liquid core extends to the wall and sprays whose atomization is completed before wall impingement will be assessed. This is of interest because of the current trends toward smaller engines and higher injection pressures, both of which promote increased wall impingement. Wall impingement processes are thought to influence NOx and soot emissions and wall heat transfer. This will be examined in the study.

PART C

An experimental program has been initiated at the University of Wisconsin with funding from Caterpillar and from DOE/ NASA-Lewis for engine experiments to generate data needed for KIVA validation. The work will comprise three tasks: 1. in-cylinder gas velocity and turbulence measurements, 2. combustion visualization experiments and 3. measurements of engine-out emissions.

In setting up the experimental program, effort has been taken to ensure that the modifications to the engine needed for optical access will be minimal so that the results will be representative of actual engines. The experiments will be conducted using dual and single intake valve configurations and with standard and re-entrant piston designs.

The in-cylinder velocity measurements will be made using Particle Image Velocimetry [45,46]. The method has already been used at the University of Wisconsin [47], and techniques for rapid data analysis are available at the ERC [48].

Combustion visualization and photography experiments will be conducted through a window that replaces one of the exhaust valves. If window fouling problems prove to be insurmountable, a radiation probe will be used that has been developed and used successfully at the ERC [49]. Engine-out particulate measurements will be made using a mini-dilution tunnel sized for the CAT engine. It is anticipated that these emission measurements will be useful in assessing the validity of KIVA's soot models.

ACKNOWLEDGEMENTS

Progress on the grant has benefited from numerous interactions with faculty and students working on related research projects at the Engine Research Center under ARO and other funding. The donation of computer time by CRAY at Mendota heights and at the San Diego Supercomputer Centers are also appreciated.

REFERENCES

1. Amsden, A. A., Ramshaw, J. D., O'Rourke, P. J. and Dukowicz, J. K., "KIVA: A Computer Program for Two- and Three-Dimensional Fluid Flows with Chemical Reactions and Fuel Sprays," Los Alamos Scientific Laboratory Report LA-10245-MS, February 1985.
2. Amsden, A. A., Butler, T. D. and O'Rourke, P. J. "The KIVA-II Computer Program for Transient Multi-Dimensional Chemically Reactive Flows with Sprays," Society of Automotive Engineers Technical Paper 872072, 1987.
3. Glikin, P.E. "Fuel Injection in Diesel Engines," Proceedings of the Institution of Mechanical Engineers, Vol. 199, No. 78, pp. 1-14, 1985.
7. Greeves, G. "Response of Diesel Combustion to Increase in Fuel Injection Rate," Society of Automotive Engineers Technical Paper 790037, 1979.
8. Greeves, G. and Wang, C.H.T. "Origins of Diesel Particulate Mass Emissions," Society of Automotive Engineers Technical Paper 810260, 1981.
6. Yoshikawa, S., Furusawa, R., Arai, M. and Hiroyasu, H. "Optimizing spray behavior to improve engine performance and to Reduce Exhaust Emissions in a Small DI Diesel Engine" Society of Automotive Engineers Technical Paper 89046, 1989.
7. Cartellieri, W.P. and Herzog, P.L. "Swirl supported or Quiescent Combustion for 1990s Heavy-Duty DI Diesel Engines - An Analysis," Society of Automotive Engineers Technical Paper 880342, 1988.
8. Siegla, D.C. and Alkidas, A.C. "Evaluation of the Potential of a Low-Heat-Rejection Diesel Engine to Meet Future EPA Heavy-Duty Emission Standards," Society of Automotive Engineers Technical Paper 890291, 1989.
9. Gonzalez D., M.A., Borman, G.L. and Reitz, R.D. "A Study of Diesel Cold Starting using both Cycle Analysis and Multidimensional Calculations," Society of Automotive Engineers Technical Paper 910180, 1991.
10. Abraham, J. and Bracco, F.V. "Fuel-Air Mixing and Distribution in a Direct-Injection Stratified-Charge Rotary Engine," Society of Automotive Engineers Technical Paper 890329, 1989.
11. Kuo, T.-W. and Reitz, R.D. "Computations of Premixed-Charge Combustion in Pancake and Pent-roof Engines," Society of Automotive Engineers Technical Paper 890670, 1989.
12. Reitz, R.D. "Three-Dimensional Modeling of Diesel Spray Combustion and Emissions," Proceedings of the DOE Automotive Technology

Development Contractors Coordination Meeting, Dearborn, MI, October 22-25, 1990, SAE P-243.
13. Reitz, R.D., and Rutland, C.J. "Three-Dimensional Modeling of Diesel Engine Intake Flow, Combustion and Emissions," Proceedings of the DOE Automotive Technology Development Contractors Coordination Meeting, Dearborn, MI, October 28-31, 1991.
14. Reitz, R.D., and Rutland, C.J. "Three-Dimensional Modeling of Diesel Engine Intake Flow, Combustion and Emissions," Society of Automotive Engineers Paper 911789, 1991.
15. Naber, J.D. and Reitz, R.D. "Modeling Engine Spray/Wall Impingement" Society of Automotive Engineers Paper 880107, 1988.
16. Gonzalez D., M.A., Borman, G.L. and Reitz, R.D. "A Study of Diesel Cold Starting using both Cycle Analysis and Multidimensional Calculations," SAE paper 910180, 1991.
17. Reitz, R.D., 'Assessment of Wall Heat Transfer Models for Premixed-Charge Engine Combustion Computations,' Submitted to Society of Automotive Engineers Transactions, SAE paper 910267, 1991.
18. Reitz, R.D. "Modeling Atomization Processes in High-Pressure Vaporizing Sprays," *Atomisation and Spray Technology*, 3, pp. 309-337, 1987.
19. Gonzalez D., M.A. and Reitz, R.D. "Modeling Diesel Engine Spray Vaporization and Combustion," Presented at the First International KIVA Users Group Meeting, Detroit, MI, February 24, 1991, and at the Fifth International Conference on Liquid Atomization and Spray Systems, NIST Gaithersburg, MD, USA, July 15-18, 1991.
20. Kamimoto, T., Yokota, H. and Kobayashi, H. "Effect of High Pressure Injection on Soot Formation Processes in a Rapid Compression Machine to Simulate Diesel Flames," Society of Automotive Engineers Paper 871610, 1987.
21. Yan, J. and Borman, G.L. "Analysis and in-cylinder measurement of particulate radiant emissions and temperature in a direct injection diesel engine," SAE Paper 881315 (1988).
22. Lei, N. "A cycle simulation program for the dynamic operation of a single cylinder direct injection diesel," MS Thesis, Department of Mechanical Engineering, University of Wisconsin-Madison (1988).
23. M. A. Gonzalez D., Z. W. Lian and R. D. Reitz, "Modeling Diesel Engine Spray Vaporization and Combustion," Submitted for publication for the 1992 SAE Congress and Exposition, Detroit, MI.
24. Z. W. Lian and R. D. Reitz, "Effect of Vaporization and Gas Compressibility on Liquid Jet Breakup," Submitted for Publication, Physics of Fluids, 1991.
25. Prosperetti, A. and Plesset, M. S., 'The Stability of An Evaporating Liquid Surface,' *Phys. Fluids* 27, **7**, 1984. pp. 1590-1602.
26. Hiquera, F. J., 'The Hydrodynamic Stability of An Evaporating Liquid,' *Phys. Fluids* 30, **3**, 1987. pp. 679-686.
27. Bradley, D. 'On the Atomization of Liquid By High-Velocity Gases,' J. *Phys. D: Appl. Phys.*, Vol. 6, 1973.

28. Bradley, D. 'On the Atomization of A Liquid by High-Velocity Gases: II,' J. *Phys. D: Appl. Phys.*, Vol. 8, 1975.
29. Priem, R. J., Borman, G. L., El-Wakil, M. M., Uyehara, O. A., and Myers, P. S., "Experimental and Calculated Histories of Vaporizing Fuel Drops", NACA TN 3988, 1957.
30. Jin, J. D., and Borman, G. L., "A Model for Multicomponent Droplet Vaporization at High Ambient Pressures", Society of Automotive Engineers paper 850264, 1985.
31. Abramazon, B., and Sirignano, W. A., "Approximate Theory of a Single Droplet Vaporization in a Convective Field", ASME/JSME Thermal Engineering Conference, Vol. 1, 1987, pp. 11-18.
32. Bergeron, C.A. and Hallett, W.L.H. "Autoignition of Single Droplets of Two-Component Liquid Fuels," *Combust. Sci. and Tech.*, **65**, pp. 181-194, 1989.
33. Abraham,J., Bracco,F.V., and Reitz,R.D., "Comparison of Computed and Measured Premixed Charged Engine Combustion", Combustion and Flame, 60, 1985.
34. Kong, S.-C., Ayoub, N., and Reitz, R.D., "Modeling Combustion in Compression Ignition Homogeneous Charge Engines," Submitted for publication for the 1992 SAE Congress and Exposition, Detroit, MI.
35. Boggs,D.E., Ph.D. Thesis, University of Wisconsin-Madison,1990.
36. Yuh,H.J., and Mirsky,W., "Schlieren-Streak Measurements of Instantaneous Exhaust Gas Velocity from a Spark Ignition Engine", Society of Automotive Engineers Paper 741015, 1974
37. Westbrook,C.K., and Dryer,F.L., *Combust. Sci. Technol.*, **20**, 125, 1979.
38. Reitz, R.D. and Kuo, T.-W. "Modeling of HC Emissions Due to Crevice Flows in Premixed-Charge Engines," Society of Automotive Engineers Paper 892085, 1989.
39. Abraham,J., William, F.A., and Bracco,F.V.,"A discussion of turbulent flame structure in premixed charges", Society of Automotive Engineers Paper 850345, 1985
40. Eaton, A.R. & Reynolds, W.C., "Flow structure and mixing in a motored axisymmetric engine," Society of Automotive Engineers Paper 890321, 1989.
41. Theobald, M.A. and Cheng, W.K. "A Numerical Study of Diesel Ignition," American Society of Mechanical Engineers Paper 87-FE-2, 1987.
42. Gentry, R.A., Daly, B.J. and Amsden, A.A. "KIVA-COAL: A Modified Version of the KIVA Program for Calculating the Combustion Dynamics of a Coal-Water Slurry in a Diesel Engine Cylinder," Los Alamos National Laboratory Report LA-11045-MS, August 1987.
43. Chang, S.L. and Rhee, K.T. "Computation of Radiation Heat Transfer in Diesel Combustion," Society of Automotive Engineers Paper 831332, 1983.
44. Menguc, M.P., Viskanta, R. and Ferguson, C.R. "Multidimensional modeling of Radiative Heat Transfer in a Diesel Engine," Society of Automotive Engineers Paper 850503, 1985.
45. Reuss, D.L., Adrian, R.J., Landreth, C.C., French, D.T. and Fansler, T.D. "Instantaneous Planar Measurements of Velocity and Large Scale Vorticity

and Strain Rate in an Engine Using Particle-Image Velocimetry," SAE Technical Paper 890616, 1989.
46. Reuss, D.L., Bardsley, M., Felton, P.G., Landreth, C.C. and Adrian, R.J. "Velocity, Vorticity, and Strain-Rate Ahead of a Flame Measured in an Engine Using Particle Image Velocimetry," SAE Technical Paper 900053, 1990.
47. Ghandi, J.B. 'Velocity Field Characteristics in a Motored Two-Stroke Ported Engine,' PhD Thesis, University of Wisconsin-Madison, 1991. See also ERC Newsletter, Vol. 4, No. 1, April 1991.
48. Goetsch, D. and Farrell, P.V. 'Optical LCTV Correlator for Particle Image Velocimetry,' *Optics Letters*, **14**, 978, (1989).
49. Yan, J. "Analysis and In-cylinder Measurements of Local and Hemispherical Particulate Radiant Emissions and Temperatures in a Direct Injection Diesel Engine," Ph.D. Thesis, University of Wisconsin, 1988.

APPENDIX 1 KIVA USERS GROUP ACTIVITY

The KIVA computer code and its predecessor codes were written at the Los Alamos National Laboratories, New Mexico [1,2]. These codes have seen increasing use by university researchers, government laboratories and engine industries in the U.S. and abroad since the early 1970s. A U.S. KIVA Users group was formed during the DOE Diesel Working Group Meeting at the University of Wisconsin-Madison in the Fall of 1989 . The purpose of this Users Group is to promote the use of KIVA and to facilitate exchange of information among KIVA users. Since that time KIVA Users Groups have also been formed in Europe and Japan.

The U.S. KIVA Users Group currently numbers about 80 organizations. We have served as the editors of the KIVA Users Newsletter and four issues have already been distributed to the membership (copies of the newsletters are attached in this Appendix). We also co-organized the First International KIVA Users Group Meeting with CRAY Research which took place in February 1991 in Detroit, MI. This meeting was attended by 75 registrants. A similar meeting is currently being planned for 1992. Details will be released in the 5th KIVA Users Newsletter later this month.

KIVA Users Group

First Newsletter --- April 1990

Questionnaire Results

Thank you for your participation in the KIVA User's Group questionnaire. The following is a brief summary of answers to the survey questions. These answers are being used for planning the User's Group.

A. Questions and Summary of Answers

In the following, the first column of numbers after an answer gives the total number of responses for that question; the second column is the percentage of the total response. For some of the questions more than one answer was possible, making the total number of responses more than fifty.

Question #1 - *Are you willing to be listed in a directory of KIVA users?*

Two hundred surveys were sent out, of which 53 were returned. Fifty of these respondents were interested in being listed in a KIVA directory.

Question #2 - *What is your application of KIVA? (More than one answer possible.)*

	#	%
1. gas turbines	7	12
2. rockets *	3	5
3. IC engines CI	18	31
4. IC engines SI	6	10
5. IC engines rotary	2	3
6. furnaces	1	2
7. general CFD**	15	25
8. not active at present	3	5
9. no answer	4	7
total	59	

* (LOX combustor analysis, liquid rocket combustion)
**(spray combustion and evolution, air motion, heat transfer, emissions)

Question #3 - *What KIVA applications might you make in the future? (More than one answer possible.)*

	#	%
1. acoustics	1	1
2. spray studies *	10	17
3. combustion **	6	10
4. heat transfer	5	8
5. IC engines	10	17
6. turbines	4	7
7. general CFD ***	6	10
8. numerical studies	2	3
9. no answer	14	23
10. not active	2	3
total	60	

* (spray combustion, droplet breakup, combustion bombs, spray evaporation)
**(emissions, plasma jet ignition, flame propagation, fuel-air mixing, hazardous waste incinerators, combustion with propane and jet-A)
*** (free surface flow, flow structure interaction, aero-optical problems, port flows, fluid dynamical instabilities, chamber geometry application, condensation of minerals in solar nebula, cylinder head port design)

Question #4 - *Does your version of KIVA contain enhancements made by your organization?*

	#	%
1. yes	24	48
2. no	22	44
3. no answer	3	6
4. other	1	2

Question #5 - *Would you be willing to share your enhancements of KIVA with others? (including reports, source codes)*

	#	%
1. yes	24	48
2. no	3	6
3. some	16	32
4. no answer	6	12
5. other	1	2

An analysis of the responses to questions #4 and #5 indicated that both those who had made enhancements during the previous year and those who had not were willing to share all or at least some of their future enhancements with the User's Group.

Question #6 - *Has your organization made any successful applications of KIVA during the year 1989?*

	#	%
1. yes	18	36
2. no	25	50
3. unfinished	2	4
4. no answer	5	10

Question #7 - *Would you be willing to document your successful applications of KIVA? (e.g., for a newsletter.)*

	#	%
1. yes	35	70
2. no	3	6
3. some	3	6
4. no answer	7	14
5. other	2	4

A comparison of questions #6 and #7 shows that the majority of respondents are willing to document their applications of KIVA, whether or not they made successful applications during 1989.

Question #8 - *Would you be interested in knowing about other successful applications of KIVA?*

	#	%
1. yes	49	98
2. no	0	0
3. no answer	1	2

A comparison of the responses to questions #7 and #8 shows that almost all respondents are interested in knowing about other successful applications, with only a small percentage unwilling to share their own.

Question #9 - *What kind of computer(s) are you using for KIVA calculations? (More than one answer possible)*

	#	%
1. mainframes*	45	57
2. vector processors**	1	1
3. super workstations***	21	27
4. personal computers	1	1
5. no answer	7	9
6. none	3	4
7. other	1	1
total	79	

*(Cray, CDC, IBM)
**(FPS 640)
***(Sun, Apollo, Decstation, Honeywell, Ardent, VAX, Alliant, Convex)

Question #10 - *What grid generation/graphics systems (software and hardware) are you using? (More than one answer possible)*

	#	%
1. commercial graphics software*	15	21
2. grid generation software**	6	8
3. graphics terminals***	10	14
4. KIVA software only	9	12
5. custom	12	16
6. not yet decided	5	7
7. no answer	13	18
8. other	3	4
total	73	

*(DI-3000, Plot 3D, Dissplа, Tecplot, 3D Grape, GPlot, NCAR, Disspop)
** (SDRC I-deas, Eagle, NCSA)
***(Sun-4, Iris, IBM, Mac, silicon graphics, Tektronix 4208, HP-plot)

Question #11 - *Which format(s) are you in favor of? (check all that apply)*

	#	%
1. newsletter	42	34
2. electronic mail	18	14
3. yearly conference for discussions	30	24
4. User's Group interaction with Society meetings	32	26
5. other	2	2
6. no answer	1	1
total	125	

Question #12 - *Would you send representatives to User Group meetings?*

	#	%
1. yes	40	80
2. no	2	4
3. maybe/probably	2	4
4. no answer	5	10
5. N/A	1	

Question #13 - *If you would send representatives to a group meeting, how many times a year would be considered maximum?*

	#	%
1. one	30	60
2. two	13	26
3. four	1	2
4. no answer	1	2
5. uncertain	5	10

Question #14 - *Would you submit short articles or notices to a newsletter?*

	#	%
1. yes	41	82
2. no	4	8
3. no answer	3	6
4. maybe/don't know	2	4

Question #15 - *Should distribution of the newsletter after the first year be restricted to those who have submitted articles during the prior year?*

	#	%
1. yes	3	6
2. no	45	90
3. no answer	1	2
4. other	1	2

Question #16 - *Should distribution of the newsletter be restricted to those who are willing to be listed in the directory?*

	#	%
1. yes	24	48
2. no	25	50
3. no answer	1	2

Question #17 - *Would you use electronic mail to transfer information about KIVA to others?*

	#	%
1. yes	24	48
2. no	19	38
3. maybe	3	6
4. no answer	2	4
5. other	2	

Question #18 - *Do you believe that enough people would submit material to allow publication of a quality newsletter?*

	#	%
1. yes	35	70
2. no	9	18
3. don't know	3	6
4. no answer	2	4
5. other	1	2

Question #19 - *Would you be willing to pay a modest fee for membership costs?*

	#	%
1. yes	38	76
2. no	8	16
3. no answer	3	6
4. probably	1	

B. Format of the User Group

This newsletter is the first of what will hopefully be a continuing series, published as new material and information warrants. According to the results of the questionnaire, 82% of you are willing to submit articles to this newsletter. Please submit any items of interest that you would be willing to share with other members of the user group.

The preferred format for the User's Group information exchange was a newsletter. The second and third choices were yearly conferences and User's Group interaction with Society meetings. It is suggested that the first KIVA Users Group meeting be held in conjunction with the 26th AIAA/SAE ASME/ASEE Joint Propulsion Conference and Exhibit, Orlando, Florida, July 16-18, 1990. Another possible meeting of KIVA Users could take place at the SAE off-highway meeting, to be held in Milwaukee this September. If you are interested in getting together at these or other meetings, please respond by U.S. mail or electronic mail.

C. KIVA Users Database

The individual questionnaire responses have been compiled into a database that is available to KIVA User Group members. For details contact Rolf Reitz.

D. KIVA Update Planned

Los Alamos is planning a release of a new version of KIVA-2 that includes repairs of minor "bugs" found in the original. This release will be distributed free-of-charge to all users recorded with the Argonne Software Support Center.

For User Group Information please direct correspondence to:
Rolf D. Reitz 123 Engineering Research Building
1500 Johnson Drive University of Wisconsin
Madison, WI 53706 Phone: (608) 262-0145
FAX: (608) 262-6707 reitz@engr.wisc.edu

KIVA Newsletter No. 1 April, 1990
Written by Kristen Becker and Rolf D. Reitz

KIVA Users Group Newsletter #2 --- July 1990 Editor: Rolf D. Reitz

New Release of KIVA-II

A new release of KIVA-II, dated 053190, is now available. All KIVA-II users on record with the National Energy Software Center will be sent the new release by NESC shortly. This new version corrects several minor bugs in the first version of KIVA-II and all users are advised to use the newer version in their future calculations.

Diffusion Flame Test Problems

Two test problems have been studied at Los Alamos with the new release of KIVA-II. The first considers the inter-diffusion of two initially-separated species in a uniform parallel flow in a 3 cm long tube with W=10 m/s and mass diffusivity D = constant. The geometry is shown in Fig. 1. Other details of the comparison are summarized in Table 1.

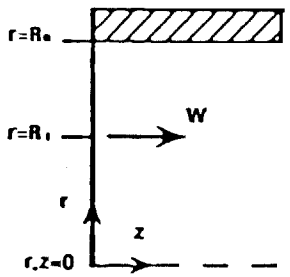

Fig. 1 *Computational Domain* (R_1=0.5, R_0=1.0 cm, W=10 m/s and D=66.7 cm^2/s)

To perform this test computation you must "turn off" the chemical reactions either by setting input parameter CF(1)=0 or TCUT=400. Plots of the computed and analytic solutions are compared in Fig. 2. The computations were made on a 20x1x30 grid and the solution is shown at 30 ms after the beginning of the computation. The high and low contour levels are L=0.1, H=0.9, respectively. The two agree very well except very near the inflow boundary. This is believed to be due to the fact that a zero normal gradient is assumed when computing diffusive fluxes at an inflow boundary (cf. p. 86 of the KIVA-II report). The error is small, but you may wish to correct it.

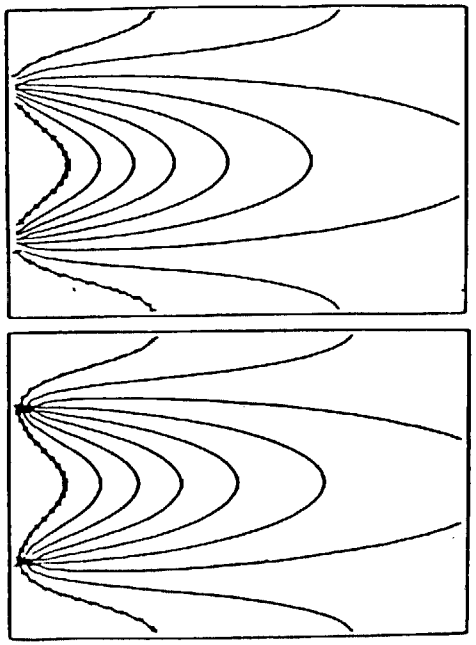

Fig. 2 *Comparison of Analytic (top) and KIVA-II solutions (bottom) for test problem 1 which considers the inter-diffusion of two initially separated species flowing in a tube.*

B.C.s: for $0 \le r \le R_1$, $Y_1 = 1, Y_2 = 0$

for $R_1 < r \le R_0$, $Y_1 = 0, Y_2 = 1$

$$\frac{\partial Y_1}{\partial r} = \frac{\partial Y_2}{\partial r} = 0 \text{ for } r = 0, r = R_0$$

Exact Solution (Steady State):

$$Y_1(r,z) = \left(\frac{R_1}{R_0}\right)^2 + \sum_{j=1}^{\infty} a_j J_0\left(r\sqrt{\frac{k_j^2}{D}}\right) e^{-m_j z}$$

where k_j^2 is determined from $J_1\left(R_0\sqrt{\frac{k_j^2}{D}}\right) = 0$,

$$m_j = \frac{\sqrt{W^2 + 4Dk_j^2} - W}{2D}, \text{ and}$$

$$a_j = \left[\sqrt{\frac{D}{k_j^2}} R_1 J_1\left(R_1\sqrt{\frac{k_j^2}{D}}\right)\right] \Big/ \left[\frac{R_0^2}{2} J_0^2\left(R_0\sqrt{\frac{k_j^2}{D}}\right)\right]$$

Table 1. *Boundary Conditions and Analytic Solution*

In the second test problem, the two species of the first problem are allowed to react at a high rate to form a product of equal molecular weight. There is no heat release associated with the reaction, and hence the flow field is still uniform. Plots of the mass fraction of the fuel and oxidizer species are shown in Fig. 3. The analytic solution for the flame location is the Y_1=0.5 contour of the solution to the first problem. Inspection of the plots shows that the Y_1=0.5 contour of problem 1 lies approximately at the boundary between the regions containing the fuel and oxidizer species in Fig. 3.

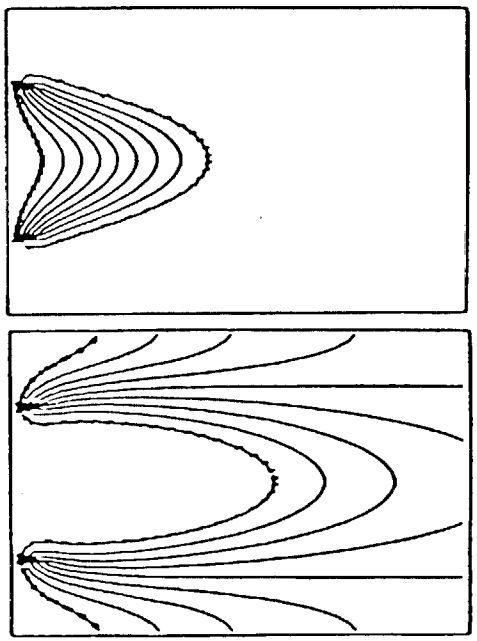

Fig. 3 *Results from test problem 2 showing KIVA-II's predicted fuel (top) and oxidizer (bottom) contours when the species of test problem 1 are allowed to react. The computations used the same grid as for problem 1 and the results are also shown at t=30 ms.*

Further details about these test problems and the new release of KIVA-II are available from Tony Amsden and Pete O'Rourke (Group T-3, MS B216, Los Alamos National Laboratory, Los Alamos, NM 87545).

Computations of Scavenging Flow In a Two-Stroke Engine

A modification of KIVA-II has been introduced by Peter Epstein at the University of Wisconsin that allows computations to be made in complex engine geometries. An example application is given in which three versions of KIVA-II are run simultaneously. Each version considers a separate block of the computational domain, and the blocks exchange boundary condition information with each other at their common interfaces. The use of separate blocks permits the connectedness of the overall computational domain to change with time. The scavenging flow in the cylinder, transfer pipes, and exhaust pipe of a ported two-stroke engine with a moving piston was modeled this way using the computational grid shown in Fig. 4

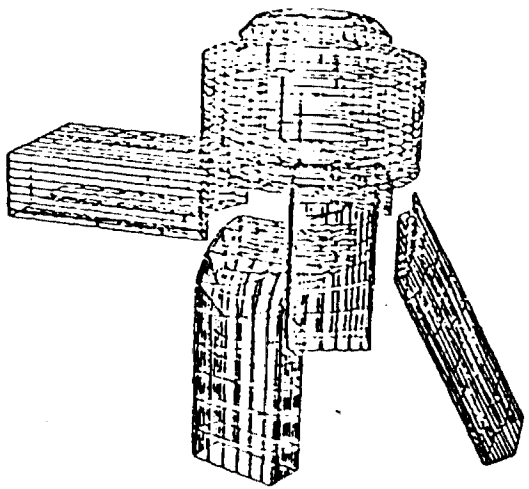

Fig. 4 A 3-D view of the computational grid for a two-stroke engine with three inlet ports (the boost inlet port on the right is inclined at a 60 degree angle) and one exhaust port (on the left). Three blocks were employed with the inlet ports represented in one block, and the exhaust port and combustion chamber in the other two. The grid is shown at 97 degrees after top dead center, just before the exhaust port opens.

Results showing details of the velocity field in the diametral plane of symmetry that includes the exhaust port and the inlet boost port are shown in Figs. 5 and 6. These computations were made with a boost port angle of 30 degrees. Figure 5 is at 133 degrees after top dead center, soon after the inlet ports have opened. There are recirculating flows at the top and the bottom of the exhaust pipe, with an exhaust jet induced by the the blow-down process in the center. The flow within the boost port is seen to be deflected by the piston. The flow travels up the cylinder wall in the region above the boost port .

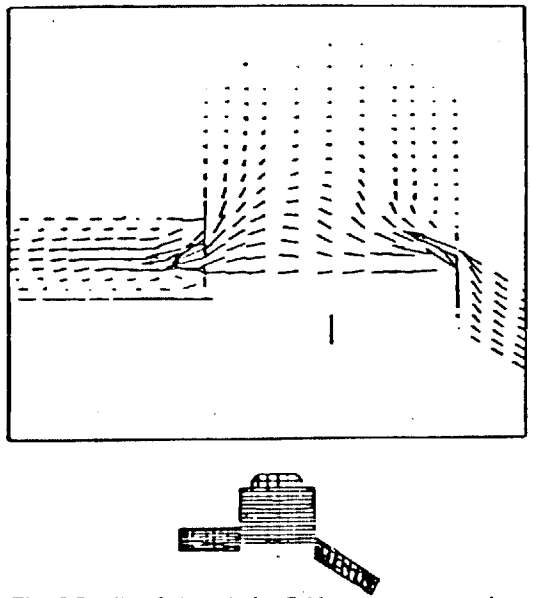

Fig. 5 Details of the velocity field on a symmetry plane through the ports and engine cylinder during the expansion stroke at 133 degrees after top dead center for an engine with an inlet boost port inclined at 30 degrees. The lone arrow pointing downward at the bottom of the figure shows the velocity scale of 100 m/s.

The exhaust flow continues throughout the scavenging process as can be seen in Fig. 6 which shows results during the compression stroke at 119 degrees before top dead center. The inlet ports are just about to close and a strong jet is seen flowing back into the boost port. A toroidal vortex is generated within the combustion chamber during the scavenging process which survives after the ports close.

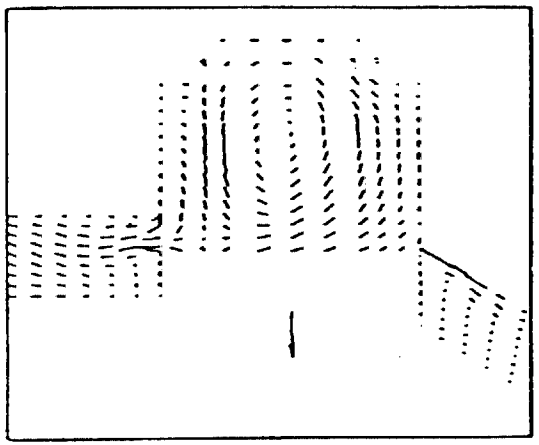

Fig. 6 Details of the velocity field on a symmetry plane through the ports and engine cylinder during the compression stroke at 119 degrees before top dead center for an engine with an inlet boost port inclined at 30 degrees. The arrow at the bottom of the figure shows the velocity scale of 100 m/s.

The calculated results indicate that velocity profiles (and flow directions) vary with time and are not uniform across the ports. Other results show that the toroidal vortices in the combustion chamber are broken up in engines geometries that have high boost port angles. This puts more fresh charge into the cylinder head dome region and the trapping efficiency increases.

Further details about these and other computations are available in Peter's M.S. thesis *A computer Simulation of the Scavenging Flow in a Two-Stroke Engine*, The University of Wisconsin, 1990.

Articles for the Newsletter

Did you like this newsletter? Newsletters will only continue if you submit articles (82% of you polled in the KIVA Users Group Questionnaire said that you would be willing to submit items to our Newsletter!).

For User Group information please direct correspondence to:
Rolf D. Reitz 123 Engineering Research Building
1500 Johnson Drive University of Wisconsin
Madison, WI 53706 Phone: (608) 262-0145
FAX: (608) 262-6707 reitz@engr.wisc.edu

KIVA Users Group Newsletter #3 --- November 1990 Editor: Rolf D. Reitz

Users Group Meeting at SAE Congress

A meeting of KIVA Users is being arranged for 2.00 pm Sunday, February 24th, 1991 at COBO-Hall, Detroit, Michigan. This time and place was chosen because it is expected that many KIVA Users will be attending the Society of Automotive Engineers Congress and Exhibition to be held in Detroit, February 25th to 29th.

The meeting will be sponsored by CRAY Research and will feature about 10 prepared presentations (short descriptions of research in progress) with lively discussions.

The presentations will end at about 6.00 pm and will be followed by a Banquet with a Keynote speaker from the Los Alamos Laboratories. A registration fee will be collected to help defray the costs of the meal and the facilities. Included in the registration fee will be a book of abstracts of the presentations which will be distributed to registrants.

If you plan to attend the meeting please contact Reza Taghavi, Cray Research (612) 683-3643 or Rolf Reitz, University of Wisconsin (608) 262-0145 so that we can plan the details of the meeting.

Call for Abstracts

KIVA Users wishing to present their research at the Users Group meeting in Detroit should submit a short abstract (maximum 5 single spaced pages including figures) to Reza Taghavi, Industry, Science & Technology Dept., Cray Research Park, 655E Lone Oak Drive, Eagan, MN 55121 by January 11th 1990. Further details about the abstract and oral presentation formats will be sent to authors later.

KIVA Descriptions and Sample Input Data Available on the UNIX MAN Facility

Unix users know the utility of the MAN command. KIVA's Epilog and a sample input data deck can now be accessed as part of the UNIX MAN facility. For details about installing these MAN pages on your computer system contact Don Curtis, Texas A & M University Supercomputer Center, College Station, TX 77843 (409) 845-6910
INTERNET: dac3541@helios.tamu.edu
BITNET: DAC3541@TAMVENUS

Improving Angular Momentum Conservation in KIVA-II

KIVA-II solves conservative difference approximations to the linear momentum equations, but because of truncation errors conservation of linear momentum does not imply conservation of angular momentum. Non-conservation of angular momentum is a common problem of compressible flow hydrodynamics codes and is one reason that special optional logic was installed in KIVA-II to conserve the component of angular momentum about the z-axis. When this option is used, however, linear momentum conservation is surrendered, and other components of the angular momentum are still not conserved.

One of the main truncation errors giving rise to non-conservation of angular momentum in KIVA-II has recently been identified by the Los Alamos group. With a simple change to the code one can greatly reduce this truncation error and thereby obtain better conservation of all components of angular momentum, without compromising linear momentum conservation and without using any special angular momentum conservation logic. The change is to replace the factor 0.25 with 0.125 in lines 73, 76 and 79 of Subroutine UFINIT.

The motivation for this study was the discovery that some KIVA-II calculations of inviscid vortices were unstable. The instability manifested itself in an unbounded increase in the angular momentum of vortices. It does not arise in viscous flow calculations, such as k-ε calculations, in which the physical viscosity is large enough to damp the destabilizing truncation errors.

An example instability is given in Fig. 1 for a calculation of the evolution of an inviscid, low Mach number flow that is initially in solid body rotation about the axis of a cylindrical vessel. The calculation was performed with quasi-second order upwind (QSOU) differencing of the convective terms and without the angular momentum logic. At time t=1.6 (non-dimensionalized by the rotation time of the initial vortex), the total angular momentum in the mesh, which is conserved in the exact solution to the differential equations, has increased to 2.06 (non-dimensionalized by its initial value).

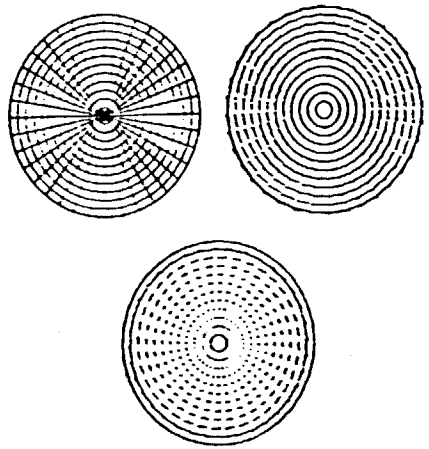

Fig. 1 *KIVA-II calculation of solid body rotation about the axis of a cylindrical vessel, using the unmodified code. Clockwise from upper left: an x-y plane of the computing mesh, the velocity vectors at time t=0 (Vmax=1.0), and at time t=1.6 (Vmax=2.39).*

Since the QSOU difference scheme is known to be stable and monotone (see Appendix M of the KIVA-II report), the source of the instability was suspected to be in the Lagrangian phase of the calculation.

Preliminary calculations showed the results were very sensitive to the magnitude of the centrifugal force term in the cell face velocity equation, Eq. (82) in the KIVA-II report. By inserting an adjustable factor f in the difference approximation to this term in Eq. (86), instability was obtained for f=1.0 (the value currently used by the code), damping of angular momentum for f=0.0, and good angular momentum conservation for f=0.5. When f=0.5 the total angular momentum at the end of the calculation of Fig. 1 was 0.92, and when f=0.0 the final value was 0.64.

To explain these results the Los Alamos group performed a discrete analysis of the finite difference equations applied to a cylindrical mesh. Assuming incompressible, axisymmetric flow, they obtained

$$\frac{V^{n+1}}{V^n} = 1 - C(\Delta\theta)^2 NS\left[\mu - C\left(f\,NS - \frac{NS-1}{2}\right)\right] + H.O.T. \quad \text{(1)}$$

where H O T stands for higher order terms, V is the azimuthal velocity at radial location r, $\Delta\theta$ is the angle determining the azimuthal cell size, $C=Vdt_s/r\Delta\theta$ is the Courant number based on the convective subcycle timestep dt_s, and NS is the number of convective subcycles each computational cycle. The factor f has been defined above, and the upwinding parameter $\mu=C/2$ (for OSOU) and $\mu=(\beta C+\alpha)/2$ (for partial donor cell differencing). (For a detailed derivation of Eq (1) contact Peter O'Rourke.) In the absence of truncation errors $V^{n+1}=V^n$. For small $\Delta\theta$ stability depends on the sign of the expression in brackets in Eq (1), the calculation will be stable if and only if

$$\mu \geq C[1/2+(f-1/2)/NS] \quad \ldots \quad (2)$$

It is seen that this formula predicts the observed behavior when OSOU differencing is used and f is varied as above. Additional calculations of the swirl problem of Fig 1 varying all parameters in Eq. (2) have corroborated the validity of this stability criterion. Based on Eq (2) it is recommend that you make f=0.5 a permanent change to KIVA-II. Taking f=0.5 corresponds to using the factor 0.125 in the calculation of the quantities DUAL, DUAF, and DUAB in Subroutine **UFINIT**.

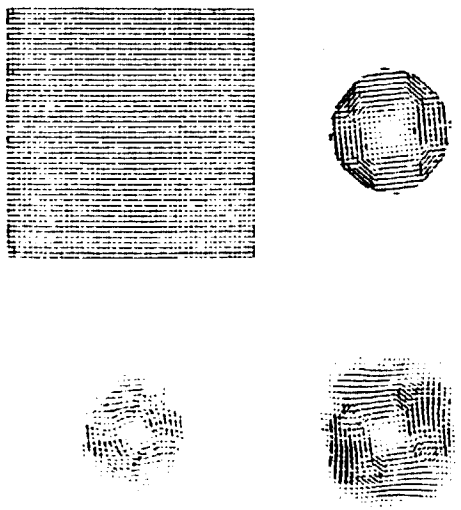

Fig. 2 *KIVA II calculation of a circular island of fluid in solid body rotation in a quiescent fluid. Upper left: the mesh of square cells. Upper right: Velocity vectors at time t=0.; Lower left: Velocity vectors at time 1.0 for the unmodified code (U_{max} 2.20). Lower right: Velocity vectors at time 1.0 for the modified code (U_{max} 1.71).*

For OSOU differencing, this choice gives the most accurate calculation of angular momentum, and for partial donor cell differencing it gives stability of the angular momentum calculation for all values of α and β for which convection of linear momentum is stable.

Although Eq (2) was derived for cylindrical meshes, the trends it predicts continue to hold for other types of meshes. Figure 2 shows initial and final velocity fields from calculations in a mesh of square cells of a circular island of fluid in solid body rotation in a quiescent fluid. When t=1.0, the total angular momentum in the mesh increases to 1.87 when t=1.0, and the total angular momentum fluctuates but never exceeds 1.06 when t=0.5.

Further details are available from Tony Amsden and Pete O'Rourke (Group T-3, MS B216, Los Alamos National Laboratory, Los Alamos, NM 87545).

Three-Dimensional Computations of Flow and Fuel Injection Flow in an Engine Intake Port

Engines with port fuel injection (PFI) systems have become popular as a means of improving vehicle performance through faster response and higher specific output. However, port fuel injection and spray vaporization details influence smoke and hydrocarbon emissions from PFI engines. The KIVA code is being used at the General Motors Research Laboratories to analyze the PFI process.

KIVA was modified to consider gas flow and fuel injection in a model engine intake port. In initial calculations the port-flow initial and boundary conditions were obtained from a single-cylinder engine simulation program and one end of the port was partially blocked to simulate gas flow through a valve annulus.

The results given in Fig. 3 show computed velocity vectors in a cutting plane through the port centerline at 350 and 340 deg BTDC firing. Hot burned gas enters the intake port as an annular jet during the back-flow period that exists immediately after the intake port opens at 380 BTDC. An extremely complicated flow pattern exists at the time of flow reversal (340 deg) which promotes mixing between the burned and fresh charge.

Figure 3 also shows the computed spray drop locations in the same plane at 270 and 230 deg BTDC. The spray can be seen to have been deflected by the strong intake gas flow. The injection ended at 230 deg BTDC and the computations predict that less than

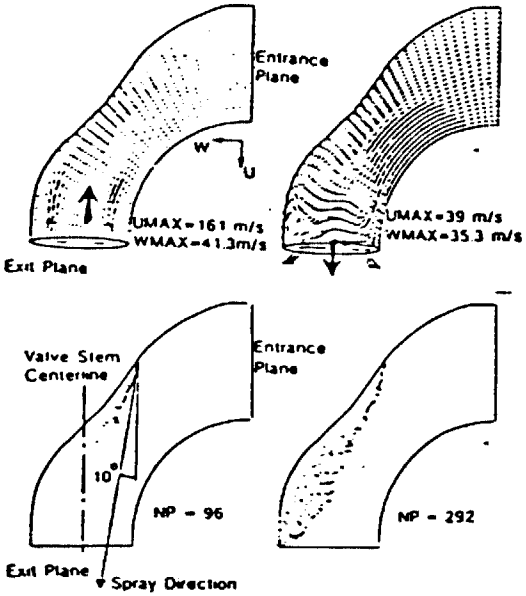

Fig. 3 *Three-dimensional computations of intake port flow and fuel injection. Top: velocity vectors in a plane through the center of the port showing details of back-flow and flow direction reversal during intake. Bottom: spray parcel locations showing the deflection of the spray.*

5% of the injected fuel has been vaporized by that time. However, port fuel vaporization details were found to be strongly influenced by the details of the mixing of fresh charge with the burned gases that occurs during the back-flow period.

These results indicate that gas flow, fuel-injection process, and port geometry have a strong influence on the details of fuel induction into the cylinder. Further information is available from Tang-Wei Kuo and Shengming Chang (Engine Research Department, General Motors Research Laboratories, Warren, MI 48090).

Articles for the Newsletter

Did you like this newsletter? Newsletters will only continue if you submit articles (82% of you polled in the KIVA Users Group Questionnaire said that you would be willing to submit items to our Newsletter!).

For User Group Information please direct correspondence to:

Rolf D. Reitz 123 Engineering Research Building
1500 Johnson Drive University of Wisconsin
Madison, WI 53706 Phone: (608) 262-0145
FAX (608) 262-6707 reitz@engr.wisc.edu

KIVA Users Group Newsletter #4 --- February 1991 Editor Rolf D Reitz

First International KIVA Users Group Meeting in Detroit at SAE Congress

A meeting of KIVA Users will be held from 2:00 6:30 pm Sunday, February 24th, 1991 in Room 814, Veterans Memorial Building, 151 West Jefferson Street (next door to COBO Hall), Detroit, Michigan. This time and place was chosen because it is expected that many KIVA Users will be attending the Society of Automotive Engineers Congress and Exhibition to be held in Detroit, February 25th to 28th.

The meeting is sponsored by CRAY Research and features 9 prepared presentations together with a Keynote speaker from the Los Alamos Laboratories. The presentations will end at 6:30 pm and will be followed by a social period (cash bar). A registration fee of $15 will be collected to help defray costs, including the book of abstracts of the presentations which will be distributed to registrants.

A Banquet will be held in the Penthouse starting at 7:00 pm. The participation fee for those wishing to attend the presentations and the Banquet is $45. A minimum of 5 days advance registration is required for the Banquet (make checks payable to Cray Research Inc.). Send advance registration material to Reza Taghavi (Industry, Science and Technology Department, Cray Research Park, 655E Lone Oak Drive, Eagan, MN 55121).

If you plan to attend the meeting please contact Reza Taghavi, Cray Research (612) 683-3643 or Rolf Reitz, University of Wisconsin (608) 262-0145 so that we can plan the details of the meeting.

KIVA Users Group Meeting Preliminary Program

Sunday, February 24, 1991
Room 814, Veterans Memorial Building
151 West Jefferson Street
Detroit, Michigan

Chairman R. Taghavi, *Cray Research Inc., Eagan, MN, USA*

2:00 Welcome and Announcements

2:15 3-D Computations of Flow and Fuel Injection in an Intake Port, T.-W. Kuo and S. Chang, *General Motors Research Laboratories, Warren, MI, USA*

2:35 On the Prediction of Diesel Engine Combustion using KIVA-II, C.A. Varnavas and D.N. Assanis, *University of Illinois, Champagne, IL, USA*

2:55 Implementation of a Fuel Spray Impingement model in KIVA-II, L. Shih and D.N. Assanis, *University of Illinois, Champagne, IL, USA*

3:15 Overview of Engine Modeling at IFP, P. Barriaud, *Institut Francais du Petrole, Rueil Malmaison, FRANCE*

3:35 KIVA-3: An Unstructured KIVA Program for Complex Geometries, A.A. Amsden, P.J. O'Rourke, D. Butler, *Los Alamos National Laboratory, Los Alamos, NM, USA*

3:55 Break

4:15 Keynote Address Ron Barks, Director of Industrial Applications Office, *Los Alamos National Laboratory, Los Alamos, NM, USA*

4:40 KIVA as Numerical Test Bench: Integrating KIVA in the Design Process, T. Saito, *Cray Research Inc., Eagan, MN, USA*

5:00 Computations with KIVA in an Indirect Injection Diesel Engine, T. Suzuki, *Mitsubishi Motors Corp., JAPAN*

5:20 On the Implementation of a Flame Sheet Model in KIVA-II, W.K. Cheng, *Massachusetts Institute of Technology, Cambridge, MA, USA*

5:40 Modeling Diesel Spray Vaporization and Combustion, M.A. Gonzalez D., *Intevep, Venezuela, S.A.* and R. Reitz, *University of Wisconsin, Madison, WI, USA*

6:00 Exhibits and Demonstrations

6:20 Closing Remarks

6:30-7:00 Social Period

7:00 Banquet

Selected Short Abstracts of Presentations to be made at the Detroit KIVA Users Group Meeting:

KIVA-3: An Unstructured KIVA Program for Complex Geometries

A A Amsden, P J O'Rourke, D Butler
Los Alamos National Laboratory

Since their introduction the original KIVA and KIVA II programs have been applied worldwide for the time dependent analysis of chemically reacting flows and fuel sprays in two and three space dimensions. Although many practical combustion systems have geometries that can be efficiently calculated with these earlier versions of KIVA, it is inefficient to model some complex geometries. Examples are diesel engine cylinders communicating with prechambers and two-stroke engine cylinders connected to intake and exhaust ports. In both earlier versions of KIVA the computing grid is a tensor-product mesh. This means that each cell is identified by an ordered triplet of indices (i,j,k), and each of these indices varies over a fixed range (e.g., i=1, ..., NXP), independent of the values of the other two indices. To model the above complex geometries a significant number of cells must be deactivated to encompass the entire region of interest. This has been successfully done by a number of KIVA users, but at a large cost in storage and computer time.

KIVA3 has been designed to overcome this inefficiency by employing an unstructured mesh that eliminates the necessity of maintaining large regions of deactivated cells, and results in a dramatic reduction in both storage and time for complex geometries. Our method uses indirect addressing, taking advantage of the fact that this construct vectorizes on present Cray systems and allows completely arbitrary connectivity of cells. Each cell is identified by a single index, and neighbor identification is carried in arrays giving the indices of neighboring cells. Cell face boundary conditions are carried in arrays in which the possibilities are fluid, solid, axis, moving, specified velocity, or pressure inflow/outflow. These arrays permit the direct connection of fluid regions in a completely seamless fashion, as there is no necessity for complicated interface logic to communicate between regions. The overall mesh is then surrounded by fictitious cells to simplify the application of inflow/outflow boundary conditions.

KIVA3 has a three part structure in which the grid generator and graphics are separated from the hydro portion of the program because, in general, users will supply their own pre- and post processors. The grid generator creates a file to be read by KIVA3 that contains all the grid coordinates, flags, connectivity arrays, and the cell face boundary condition arrays. KIVA3 completes the setup by sorting the storage, generating all other arrays required to describe the problem, and creating the boundary condition tables. KIVA3 writes an output file to be used by a graphics post processor.

3-D Computations of Flow and Fuel Injection in an Engine Intake Port

T-W Kuo and S Chang
General Motors Research Laboratories

Engines with port fuel injection (PFI) systems have become popular as a means of improving vehicle performance through faster response and higher specific output. However, port fuel injection and spray vaporization details influence smoke and hydrocarbon emissions from PFI engines. The KIVA code is being used at the General Motors Research Laboratories to analyze the PFI process.

On the Implementation of a Flame Sheet Model in KIVA-II

W K Cheng Massachusetts Institute of Technology

A combustion model based on the flame surface area per unit volume for premixed flame combustion in spark ignition engines, and diffusion flame in gas turbine burners has been implemented into the KIVA-II computer program. The physics of the model and the application will be discussed at the SAE meeting. The details of the implementation of the will be discussed at the KIVA Users meeting.

KIVA as Numerical Test Bench: Integrating KIVA in the Design Process.

T Saito, Cray Research

A wide range of real engine geometries can be modeled with KIVA2. Even inlet ports can be modeled with its structured mesh (the extra memory required is often more than compensated for by a high level of computational efficiency). The addition of pre- and post-processors, the enhancement of KIVA2's geometric capabilities along with the ability to read externally generated meshes makes this code an effective engine design guide.

Modeling Diesel Engine Spray Vaporization and Combustion

M. A. Gonzalez D. Intevep S.A., Venezuela
R. D. Reitz, University of Wisconsin

Diesel engine in-cylinder processes have been modeled with particular attention to spray development, vaporization, fuel/air mixture formation and combustion in conditions of high temperature and high pressure. Spray calculations in high temperature environments were found to underpredict measured gas phase penetration and this reduces the accuracy of engine combustion predictions considerably. Details of the vaporization model and effects due to numerical error were unable to explain the low spray penetrations. The size of the injected drops was found to have the most influence on the spray penetration and combustion (see Fig. 1). These results suggest that improved atomization models are needed for engine conditions.

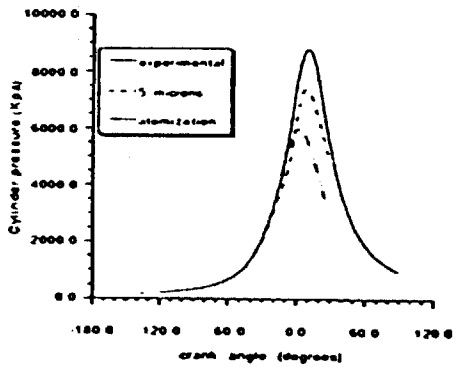

Fig. 1 Calculated and experimental cylinder pressures for a Cummins NH diesel engine showing the sensitivity to spray drop size by a) using a drop breakup model to predict injected drop size b) injecting instead a fixed drop size of 5 μm radius.

Articles for the Newsletter

Did you like this newsletter? Newsletters will only continue if you submit articles (82% of you polled in the KIVA Users Group Questionnaire said that you would be willing to submit items to our Newsletter!).

For User Group information please direct correspondence to:
Rolf D. Reitz, 123 Engineering Research Building
1500 Johnson Drive, University of Wisconsin
Madison, WI 53706, Phone: (608) 262-0145
FAX: (608) 262-6707, reitz@engr.wisc.edu

APPENDIX 2 LIST OF RELATED PUBLICATIONS AND ABSTRACTS

(papers 1 and 4-8 partially funded under grant NAG 3-1087)

1. Reitz, R.D. "Assessment of Wall Heat Transfer Models for Premixed-Charge Engine Combustion Computations," Accepted for publication in SAE Transactions, SAE Paper 910267.

Two-dimensional computations of premixed-charge engine combustion were made using the KIVA-II code. The purpose of the study was to assess the influence of heat transfer and turbulence model boundary conditions on engine combustion predictions. Combustion was modeled using a laminar- and turbulent-characteristic-time model. Flow through the piston-cylinder-ring crevice was accounted for using a phenomenological crevice-flow model. The predictions were compared to existing cylinder pressure and wall heat transfer experimental data under motoring and fired conditions, at two engine speeds. Two different wall heat transfer model formulations were considered. The first is the standard wall function method. The second is based on solutions to the one-dimensional unsteady energy equation, formulated such that the standard wall function method is recovered in the quasi-steady limit. Turbulence was modeled using the standard k-ε turbulence model equations. However, the turbulence model boundary conditions were modified to account for compressibility effects by using a coordinate transformation in the wall region. The results show that the details of wall heat transfer and turbulence model boundary conditions influence heat transfer predictions greatly through their influence on the flame speed and the flame structure in the vicinity of the wall. Inclusion of compressibility and unsteadiness effects leads to increased wall heat flux values that agree better with measurements.

2. Epstein, P., Reitz, R.D. and Foster, D. "Computations of Two-Stroke Engine Cylinder and Port Scavenging Flows," Accepted for publication in SAE Transactions, SAE paper 910672.

A modification of the computational fluid dynamics code KIVA-II is presented that allows computations to be made in complex engine geometries. An example application is given in which three versions of KIVA-II are run simultaneously. Each version considers a separate block of the computational domain, and the blocks exchange boundary condition information with each other at their common interfaces. The use of separate blocks permits the connectedness of the overall computational domain to change with time. The scavenging flow in the cylinder, transfer pipes (ports), and exhaust pipe of a ported two-stroke engine with a moving piston was modeled in this way. Results are presented for three engine designs that differ only in the angle of their boost ports. The calculated flow fields and the resulting fuel distributions are shown to be markedly different with the different geometries. The calculated results indicate that: velocity profiles vary with time and are not uniform across the ports; boost port flow at high boost angles breaks up the toroidal vortices in the cylinder that are generated by the side ports and puts more fuel into the cylinder head dome and; trapping efficiency increases with increased boost angle. These results suggest that the computational methods developed in this work will be useful as a design tool for assessing the influence of engine design parameters on scavenging efficiencies in two-stroke engines.

3. Gonzalez D., M.A., Borman, G.L. , and Reitz, R.D. "A Study of Diesel Cold Starting using both Cycle Analysis and Multidimensional Calculations," Accepted for publication in SAE Transactions, SAE paper 910180.

The physical in-cylinder processes and ignition during cold starting have been studied using computational models, with particular attention to the influences of blowby, heat transfer during the compression stroke, spray development, vaporization and fuel/air mixture formation and

ignition. Two different modeling approaches were used. A thermodynamic zero dimensional cycle analysis program in which the fuel injection effects were not modeled, was used to determine overall and gas exchange effects. The three-dimensional KIVA-II code was used to determine details of the closed cycle events, with modified atomization, blowby and spray/wall impingement models, and a simplified model for ignition. The calculations were used to obtain an understanding of the cold starting process and to identify practical methods for improving cold starting of direct injection diesel engines. It was found that, blowby gas flow represents an important source of reductions for the cylinder gas temperature at lower cranking speeds, opposing the squish flow. Overfueling and advanced injection increase the amount of fuel evaporated. The spray intact core is extended at low temperatures, spray wall impingement phenomena are characterized by low impact velocities and the bouncing of liquid drops enhances the limited fuel-air mixture formation. Failure to achieve successful ignition at low initial air temperatures was predicted by the simple kinetics model.

4. Reitz, R.D. and Rutland, C.J. "3-D Modeling of Diesel Engine Intake Flow Combustion and Emissions," SAE Paper 911789.

Manufacturers of heavy-duty diesel engines are facing increasingly stringent, emission standards. These standards have motivated new research efforts towards improving the performance of diesel engines. The objective of the present program is to develop a comprehensive analytical model of the diesel combustion process that can be used to explore the influence of design changes. This will enable industry to predict the effect of these changes on engine performance and emissions. A major benefit of the successful implementation of such models is that engine development time and costs would be reduced through their use. The computer model is based on the three-dimensional KIVA-II code, with state-of-the-art submodels for spray atomization, drop breakup/coalescence, multi-component fuel vaporization, spray/wall interaction, ignition and combustion, wall heat transfer, unburned HC and NOx formation, and soot and radiation. The accuracy of the predictions is assessed by comparison with available experimental data. Improved combustion, wall heat transfer and spray/wall impingement submodels have been implemented in KIVA during the first year activity. In addition, work is in progress on a revised atomization model, since preliminary results show that existing atomization models are inaccurate under conditions of high gas temperature and pressure (e.g., turbocharged conditions). Finally, a methodology is being developed for modeling the intake flow process to provide more realistic initial conditions for engine computations.

5. M. A. Gonzalez D. and R. D. Reitz, "Modeling Diesel Engine Spray Vaporization and Combustion," Proceedings of ICLASS-91, NIST, Gaithersburg, MD., July, 1991.

Diesel engine in-cylinder processes have been studied using computational models with particular attention to spray development, vaporization, fuel/air mixture formation and combustion in conditions of high temperature and high pressure. A thermodynamic zero-dimensional cycle analysis program was used to determine initial conditions for multidimensional calculations. A modified version of the time-dependent, three-dimensional computational fluid dynamics code KIVA-II, with a detailed treatment for the spray calculations and a simplified model for ignition, was used to determine details of the closed cycle events. These calculations were used to obtain an understanding of the potential predictive capabilities of the models. It was found that there is a strong sensitivity of the spray calculations to numerical grid resolution. However, if proper grid resolution is used, the spray calculations were found to reproduce experimental data adequately for non-vaporizing sprays. However, for vaporizing sprays in high temperature engine environments the computations underpredicted measured gas phase (vapor) penetration results substantially.

This underprediction of spray penetration reduces the accuracy of combustion predictions greatly. The atomization drop size was found to be a key parameter influencing spray penetration predictions and this indicates that improved atomization models are needed for engine conditions.

6. Z. W. Lian and R. D. Reitz, "Effect of Vaporization and Gas Compressibility on Liquid Jet Breakup," Submitted for Publication, Physics of Fluids, 1991.

A linear stability analysis is presented for an evaporating jet. The development of the surface hydrodynamic instability is assumed to be much faster than the surface evolution due to evaporation. The process is then considered as quasi-steady, and the normal mode method for the steady basic solution is applicable as an approximation. It is found that for low speed jets undergoing Rayleigh breakup, jet surface evaporation is a destabilizing factor while for high speed atomizing jets, surface evaporation becomes stabilizing. This is due to the fact that the evaporation flux distributions at the troughs and crests of the waves on the surface of the liquid jet are different for these two cases. The effect of gas compressibility is also analyzed. For subsonic jets, the maximum growth rate and the corresponding wavenumber is underestimated by neglecting the gas compressibility since the gas pressure and gas density at the interface is higher than that predicted by the conventional incompressible gas theory.

7. M. A. Gonzalez D., Z. W. Lian and R. D. Reitz, "Modeling Diesel Engine Spray Vaporization and Combustion," Submitted for publication for the 1992 SAE Congress and Exposition, Detroit, MI.

Diesel engine in-cylinder combustion processes have been studied using computational models with particular attention to spray development, vaporization, fuel/air mixture formation and combustion in conditions of high temperature and high pressure. A thermodynamic zero-dimensional cycle analysis program was used to determine initial conditions for the multidimensional calculations. A modified version of the time-dependent, three-dimensional computational fluid dynamics code KIVA-II, with a detailed treatment for the spray calculations and a simplified model for combustion, was used for the computations. These calculations were used to obtain an understanding of the potential predictive capabilities of the models. It was found that there is a strong sensitivity of the results to numerical grid resolution. However, with proper grid resolution, the calculations were found to reproduce experimental data for non-vaporizing and vaporizing sprays. However, for vaporizing sprays in high temperature engine environments with combustion, extremely fine grids are indicated. Computations made with the coarse grid sizes that are typically used underpredict measured gas phase (vapor) penetration results substantially. This underprediction of spray penetration reduces the accuracy of combustion predictions greatly. A study was made of factors that cause the observed sensitivity of the results to grid size in highly vaporizing sprays. The atomization drop size and the fuel vaporization rate were found to be key parameters that influence spray penetration predictions. Models for the processes that influence these parameters such as atomization, vapor diffusion and condensation processes are discussed.

8. Kong, S.-C., Ayoub, N., and Reitz, R.D., "Modeling Combustion in Compression Ignition Homogeneous Charge Engines," Submitted for publication for the 1992 SAE Congress and Exposition, Detroit, MI.

The combustion mechanism in a Compression Ignition Homogeneous Charge (CIHC) engine was studied. Previous experiments done on a four-stroke CIHC engine were modeled using the KIVA-

II code with modifications to the combustion, heat transfer, and crevice flow submodels. A laminar and turbulent characteristic time combustion model that has been used for spark-ignited engine studies was extended to allow predictions of ignition. The rate of conversion from one chemical species to another is modeled using a characteristic time which is the sum of a laminar (high temperature) chemistry time, an ignition (low temperature) chemistry time, and a turbulence mixing time. The ignition characteristic time was modeled using data from elementary initiation reactions and has the Arrhenius form. It was found to be possible to match all engine test cases reasonably well with one set of combustion model constants. Combustion was found to be controlled by chemical kinetic rates up to the time of ignition. After ignition, comparisons between measured cylinder pressure data and predicted pressures showed that good levels of agreement were *not* possible unless the turbulent mixing time scale was included in the combustion model. This important result implies that turbulent mixing, flame stretch and partial extinction phenomena control the rate of combustion after ignition, even in this engine that is characterized by homogeneous mixtures and the absence of a propagating flame. Ignition is controlled at low temperatures by the ignition time scale. The high temperature laminar chemistry never plays a role in determining the combustion rate since it is generally smaller than the other characteristic times. The combustion regime is classified as being between the reaction sheet and distributed reaction combustion.

9. Kuo, T.-W. and Reitz, R.D., "Three-Dimensional Computations of Combustion in Premixed-Charge and Fuel-Injected Two-Stroke Engines, " Submitted for publication for the 1992 SAE Congress and Exposition, Detroit, MI.

Combustion and flow were calculated in a spark-ignited two-stroke crankcase-scavenged engine using a laminar and turbulent characteristic time combustion submodel in the three-dimensional KIVA code. Both premixed-charge and fuel-injected cases were examined. A multi-cylinder engine simulation program was used to specify initial and boundary conditions for the computation of the scavenging process. A sensitivity study was conducted using the premixed-charge engine data. The influence of different port boundary conditions on the scavenging process was examined. At high delivery ratios, the results were insensitive to variations in the scavenging flow or residual fraction details. In this case, good agreement was obtained with the experimental data using an existing combustion submodel, previously validated in a four-stroke engine study. However, at low delivery ratios, both flow-filed and combustion-model details were important, and the agreement with experiment was poor using the existing combustion submodel, which does not account for the effect of residual gas concentration. To improve the agreement between modeling and experimental results, a modified combustion submodel was introduced that includes the effect of residual gas concentration on the laminar characteristic time. With the new submodel, agreement with the experiment has been improved considerably for all cases considered in this study. These levels of agreement between experiment and computations are similar to those found in previous applications of the laminar and turbulent characteristic-time combustion submodel to four-stroke engine combustion. Further improvement of the combustion submodel was made difficult by the observed coupling between the in-cylinder flow-field and the combustion-model details at low delivery ratios.

APPENDIX 3 FORTRAN SUBROUTINES

The three FORTRAN subroutines given in this appendix have been tested for diesel sprays (without combustion) (subroutines atomize and walint), and for premixed-charge spark-ignited engine combustion (subroutine chemprn), to date. The subroutines need to be compiled and linked together with the standard KIVA subroutines. Where noted they replace existing KIVA subroutines.

Subroutine atomize (replaces KIVA subroutine break)

This subroutine is called from the main program. It computes drop breakup by modeling the atomization process using results from a stability analysis of liquid jets. The model equations and implementation details are described in Ref [18].

Subroutine walint (new subroutine to compute spray/wall impingement)

This subroutine computes the interaction of a drop and a wall following the models and equations given in Refs. [15] and [16]. It should be called in subroutine pmove after the call to pfind for those drops that have left the domain (i.e., imom=10000).

Subroutine chemprn (replaces KIVA subroutine chem)

This subroutine is based on the laminar and turbulent characteristic time 'Princeton' combustion model used in Refs. [11,33] and [34]. The chemistry model constants are currently setup for propane fuel. References [11,33 & 34] should be consulted for details of model constants for other fuels. The subroutine also contains the Zeldo'vich NOx model as given by J.B. Heywood, Prog Energy Comb. Sci., Vol. 1, p. 135, 1976.

```
      subroutine atomize
      include 'comd.com'
      include 'part.com'
C +++
C +++ ATOMIZATION MODEL - BASED ON STABILITY OF LIQUID JETS
C +++  SEE REITZ ATOMISATION AND SPRAY TECHNOLOGY PAPER
C +++
      CNST1=0.188
      CNST2=10.0
      ALPHA=0.61
     NPP = NP
C +++
      DO 100 N=1,NP
      IMOM=I4MOM(N)
     TDROP=TP(N)
     IF(IMOM.GT.99999 .OR. TDROP.GE.TCRIT) GO TO 100
      RELVEL(N)=SQRT((U(IMOM)+UTRB(N)-UP(N))**2
     1             +(V(IMOM)+VTRB(N)-VP(N))**2
     2             +(W(IMOM)+WTRB(N)-WP(N))**2)
     IF(RELVEL(N).EQ.0.0) GO TO 100
C +++
      SURTEN= max (STM*TDROP+STB,1.E-6)
      I4=I4P(N)
    RDROP=RADP(N)
    DROPN=PARTN(N)
     WEBER =RELVEL(N)**2*RDROP/SURTEN
    WEBERG=RO(I4)*WEBER
    WEBERL=RHOP *WEBER
      TB=TDROP*0.1
      ITB=INT(TB)
      FR=TB-FLOAT(ITB)
       VISCP=FR*VISLIQ(ITB+2)+(1.0-FR)*VISLIQ(ITB+1)
      VISCP= max (VISCP,1.E-10)
     XNU   =VISCP/RHOP
    REYNOL =RDROP*RELVEL(N)/XNU
    OHN   = SQRT(WEBERL)/REYNOL
    TAYLOR = OHN*SQRT(WEBERG)
     FREQ   = SQRT(SURTEN/(RHOP*RDROP**3))
C:::::: FROM JET STABILITY DISPERSION RELATIONSHIP CURVE-FIT ::::::::::
       DENOM   = (1.+0.865*WEBERG**1.67)**0.6
         WAVLNG  =  9.02*(1.+0.45*OHN**0.5)*(1.+0.4*TAYLOR**0.7)/DENOM
    WAVLNG = WAVLNG*RDROP
        GROWTH  =  (0.34+0.385*WEBERG**1.5)/((1.+OHN)*(1.+1.4*TAYLOR**0.6))
    GROWTH = GROWTH*FREQ
      TSHATT    = 3.788*CNST2*RDROP/(GROWTH*WAVLNG)
     IF (WAVLNG.LT.RDROP/ALPHA) GO TO 40
     IF (TBREAK(N).LE.0.) GO TO 100
     TBREAK(N) = TBREAK(N) + DT
     IF (TBREAK(N).LT.TSHATT) GO TO 100
C:::::: ENLARGE DROP ONE TIME ONLY ::::::::::::::::::::::::::::::::
     TBREAK(N) = 0.
      RADEQ2    = (3.*PIO2*RDROP*RDROP*RELVEL(N)/GROWTH)**0.333333
      RADEQ1    = (0.75*WAVLNG*RDROP*RDROP)**0.33333
    RADP(N)  =  min (RADEQ1,RADEQ2)
```

```
      PARTN(N)  = DROPN*RDROP**3/RADP(N)**3
     GO TO 100
C::::::  BREAK-UP  DROP  ::::::::::::::::::::::::::::::::::::::::::::::::
  40 CONTINUE
     RADEQB   = ALPHA*WAVLNG
     DTSHAT   = DT/TSHATT
C +++
      RADP(N)=(RDROP+DTSHAT*RADEQB)/(1.+DTSHAT)
       PARTN(N)=DROPN*RDROP**3/RADP(N)**3
C +++
     IF (XDROPN(N).EQ.0.) SHEDMS(N) = 0.
      SHEDMS(N)   = SHEDMS(N) - DROPN*PI4O3R*(RADP(N)**3-RDROP**3)
     IF (XDROPN(N).EQ.0.) XDROPN(N) = DROPN
      IF (SHEDMS(N).LT.0.03*PMINJ) GO TO 100
C :: CREATE NEW PARCEL IF IT IS BIG ENOUGH AND IT HAS ENOUGH DROPS ::
      PARTNP    = SHEDMS(N)/(PI4O3R*RADEQB**3)
     IF (PARTNP.LT.XDROPN(N)) GO TO 100
     PARTN(N)  = XDROPN(N)
     XDROPN(N) = 0.
     NPP       = NPP + 1
     XDROPN(NPP) = 0.
     TBREAK(NPP) = 0.
     RADP(NPP)  = RADEQB
     RADPP(NPP)  = RADP(NPP)
     PARTN(NPP)  = PARTNP
C :::::::: CHANGE DROP VELOCITY.  HERE, V1 IS A VECTOR ORTHOGONAL
C +++       TO UREL, N1 IS A UNIT VECTOR IN DIRECTION OF V1, V2
C +++       IS A 2ND VECTOR ORTHOGONAL TO UREL AND N1, AND N2 IS
C +++       A UNIT VECTOR IN DIRECTION OF V2
     URELX=UP(N)-(U(IMOM)+UTRB(N))
     URELY=VP(N)-(V(IMOM)+VTRB(N))
     URELZ=WP(N)-(W(IMOM)+WTRB(N))
      RRELVL=URELX/(RELVEL(N)**2+1.E-20)
     V1X=1.0-RRELVL*URELX
     V1Y=0.0-RRELVL*URELY
     V1Z=0.0-RRELVL*URELZ
     V1Y=CVMGT(1.0,V1Y,V1X.EQ.0.0 .AND. V1Y.EQ.0.0 .AND. V1Z.EQ.0.0)
         RV1=1.0/SQRT(V1X**2+V1Y**2+V1Z**2)
     EN1X=V1X*RV1
     EN1Y=V1Y*RV1
     EN1Z=V1Z*RV1
     V2X=URELY*EN1Z-URELZ*EN1Y
     V2Y=URELZ*EN1X-URELX*EN1Z
     V2Z=URELX*EN1Y-URELY*EN1X
     IF(URELX.EQ.0.0 .AND. URELY.EQ.0.0 .AND. URELZ.EQ.0.0) THEN
       V2X=0.0
       V2Y=1.0
       V2Z=0.0
     ENDIF
         RV2=1.0/SQRT(V2X**2+V2Y**2+V2Z**2)
     EN2X=V2X*RV2
     EN2Y=V2Y*RV2
     EN2Z=V2Z*RV2
C +++
```

```
C +++ TO DETERMINE VELOCITY DIRECTION, INCREMENT NORMAL TO DROP PATH.
C +++ DELV IS MAGNITUDE OF VELOCITY CHANGE
C +++
      DELV=CNST1*WAVLNG*GROWTH
        THV=PI2*FRAN(0.)
      COSTHV=COS(THV)
      SINTHV=SIN(THV)
       UP(NPP)=UP(N)+DELV*(COSTHV*EN1X+SINTHV*EN2X)
       VP(NPP)=VP(N)+DELV*(COSTHV*EN1Y+SINTHV*EN2Y)
       WP(NPP)=WP(N)+DELV*(COSTHV*EN1Z+SINTHV*EN2Z)
C +++
       TP(NPP)    = TP(N)
       XP(NPP)    = XP(N)
       YP(NPP)    = YP(N)
       ZP(NPP)    = ZP(N)
       I4P(NPP)   = I4
       I4MOM(NPP) = I4
      UTRB(NPP)   = UTRB(N)
      VTRB(NPP)   = VTRB(N)
      WTRB(NPP)   = WTRB(N)
      TURBT(NPP)  = TURBT(N)
     SPDRAG(NPP) = SPDRAG(N)
     RELVEL(NPP) = RELVEL(N)
C_____________________________________________________________________
C +++ DROPLET COLLISION (O'ROURKE MODEL) APPLIED TO THE SHED DROPS
C +++ CONTAINED IN A SWEPT VOLUME = 4 PI RDROP**2 RLVL DTSHED.
C +++ XNCOLL IS THE PROBABLE TOTAL NUMBER OF COLLISIONS BETWEEN A
C +++ COLLECTOR DROP WITH THE OTHER N IN THE PARCEL IN TIME DTSHED.
C +++ XNCBAR IS THE PROBABLE NUMBER OF COLLISIONS THE COLLECTOR
C +++ DROP EXPERIENCES DURING THE TIME INTERVAL DTSHED.
C +++ PNOCOL IS THE PROBABILITY OF NO COLLISIONS.
C +++
      SUMRAD =  2.*RADP(NPP)
C +++ XNCOLL =   1.*PARTN(NPP)*RVOL*PI*SUMRAD**2*RLVL*DTSHED
C +++ XNCBAR =  XNCOLL/1.
       XNCOLL =  PARTN(NPP)*(SUMRAD/RDROP)**2
     XNCBAR =  XNCOLL
     PNOCOL =  0.
C     PNOCOL=EXP(-XNCBAR)
     IF (XNCBAR.LT.100.) PNOCOL=EXP(-XNCBAR)
     PNOCOL= max (PNOCOL,1.0E-06)
      XX=FRAN(0.)
    IF(XX.LE.PNOCOL) GO TO 60
C +++ COLLISION OCCURS, ECOAL IS THE PROBABILITY OF COALESCENCE
      FGAM=1.3
     WECOL=RHOP*RELVEL(NPP)*RELVEL(NPP)*RADP(NPP)/SURTEN
       ECOAL= min (1.,2.4*FGAM/(WECOL+1.E-20))
      YY=FRAN(0.)
    IF(YY.GT.ECOAL) GO TO 60
C +++ CASE 1: COALESCENCE
    ZZ=PNOCOL
    VNU=XNCBAR*PNOCOL
     DO 20 NK=2,1000
    ZZ=ZZ+VNU
```

```
      IF(ZZ.GE.XX) GO TO 30
       VNU=VNU*XNCBAR/FLOAT(NK)
   20 CONTINUE
   30 COLLN=FLOAT(NK-1)
C +++ PROHIBIT MORE COLLISIONS THAN ARE PHYSICALLY POSSIBLE
      IF(COLLN.GE.PARTN(NPP)) COLLN=PARTN(NPP)-1.
       RATIO  = PARTN(NPP)/(PARTN(NPP)-COLLN)
        XX     = RATIO*RADP(NPP)**3
          RADP(NPP)=(XX)**0.3333333333333333
   60 CONTINUE
      RADPP(NPP)  = RADP(NPP)
        PARTN(NPP)  = SHEDMS(N)/(PI4O3R*RADP(NPP)**3)
      SHEDMS(N)    = 0.
      SHEDMS(NPP)  = 0.
C_____________________________________________________________________
  100 CONTINUE
      NP  = NPP
     RETURN
      END
```

```
      subroutine walint
c
c         include test for the weber number of drops impinging a surface,
c         based on least square aproximation to the experimental
c         results of Wachters and Westerling.
c         October,  1989.
c
      include 'comd.com'
       include 'part.com'
      kpsq = kho(nho)
       if (nho.eq.0) kpsq=nzp
      KPSQ1= KPSQ - 1
c
        if (radp(npn).le.0.) return
      WALHIT(NPN)=WALHIT(NPN)+1.0
C  :::
C ::: CALCULATE THE INWARD NORMAL TO THE WALL AND DEFINE (XPOINT,YPOINT,
C ::: ZPOINT AS A POINT ON THE WALL.
C  :::
      I4=I4P(NPN)
       I=ITAB(I4)
       J=JTAB(I4)
      K=KTAB(I4)
      I1=I4+1
      I2=I1+NXP
      I3=I4+NXP
      I8=I4+NXPNYP
       I5=I8+1
      I6=I5+NXP
      I7=I8+NXP
     WPIST=WPISTN
     IF (K.GT.KPTOP) WPIST=0.
C ::: FOR K=1
     KPED = 1
     IPED = 1
     IF (I.GE.IPED) KPED = 1
     ITOP = 0
     IBOT = 0
    IF (K.EQ.KPED.OR.K.EQ.KPTOP) IBOT=1
    IF (K.EQ.NZ.OR.K.EQ.KPSQ1)  ITOP=1
C    IF(K.EQ.KPED.AND.F(I1).NE.0.0) THEN
     IF(IBOT.EQ.1.AND.F(I1).NE.0.0) THEN
C
C                              /3\
C                              3--3 ---/ 2
C                            /  3   /
C                            /_______/
C                       4          1
       XPOINT=X(I2)
       YPOINT=Y(I2)
      ZPOINT=Z(I2)
        XA=X(I2)-X(I4)
        YA=Y(I2)-Y(I4)
        ZA=Z(I2)-Z(I4)
```

```
      XB=X(I3)-X(I1)
      YB=Y(I3)-Y(I1)
      ZB=Z(I3)-Z(I1)
C ::: FOR THE BOTTOM CORNER CELL
C    ELSE IF(K.EQ.KPED) THEN
     ELSE IF(IBOT.EQ.1) THEN
C                          __
C                          3\     /3 6
C                           \   / 3
C                             V/ 53
C                           3-/  3--3 2
C                           //    3 /
C                           /_____3/
C                     4           1
      XPOINT=X(I6)
      YPOINT=Y(I6)
      ZPOINT=Z(I6)
        XA=X(I6)-X(I4)
        YA=Y(I6)-Y(I4)
        ZA=Z(I6)-Z(I4)
        XB=X(I3)-X(I5)
        YB=Y(I3)-Y(I5)
        ZB=Z(I3)-Z(I5)
C ::: FOR TOP WALL K=NZ OR K=KPSQ1
     ELSE IF(ITOP.EQ.1.AND.F(I1).NE.0.0) THEN
C
C                             7-------/ 6
C                           /   3   /
C                           /_______/
C                     8     3   5
C                             \3/
      XPOINT=X(I6)
      YPOINT=Y(I6)
      ZPOINT=Z(I6)
        XA=X(I6)-X(I8)
        YA=Y(I6)-Y(I8)
        ZA=Z(I6)-Z(I8)
        XB=X(I5)-X(I7)
        YB=Y(I5)-Y(I7)
        ZB=Z(I5)-Z(I7)
C ::: FOR THE TOP CORNER CELL
     ELSE IF(ITOP.EQ.1) THEN
C                           7 _______
C                           /       /3 6
C                          /       / 3
C                           8 /-------/ 53
C                             \   3---3 2
C                           / \  3   /
C                          /     3 /
C                         3/      3/1
C                         --
      XPOINT=X(I2)
      YPOINT=Y(I2)
      ZPOINT=Z(I2)
```

```
          XA=X(I2)-X(I8)
          YA=Y(I2)-Y(I8)
          ZA=Z(I2)-Z(I8)
          XB=X(I1)-X(I7)
          YB=Y(I1)-Y(I7)
          ZB=Z(I1)-Z(I7)
C ::: FOR CONSTANT I WALL
      ELSE
C
C                              /3 6
C                            5  / 3
C                            <------3- 3
C                              3----3--3 2
C                           /     3 /
C                           /_____3/
C                      4          1
        XPOINT=X(I5)
        YPOINT=Y(I5)
        ZPOINT=Z(I5)
          XA=X(I5)-X(I2)
          YA=Y(I5)-Y(I2)
          ZA=Z(I5)-Z(I2)
          XB=X(I6)-X(I1)
          YB=Y(I6)-Y(I1)
          ZB=Z(I6)-Z(I1)
      END IF
        XNORM=YA*ZB-ZA*YB
        YNORM=ZA*XB-XA*ZB
        ZNORM=XA*YB-YA*XB
         SNORM=SQRT(XNORM**2+YNORM**2+ZNORM**2)
      XNORM=XNORM/SNORM
      YNORM=YNORM/SNORM
      ZNORM=ZNORM/SNORM
c
      UPREL=UP(NPN)
      VPREL=VP(NPN)
      WPREL=WP(NPN)-WPIST
      QDOTN=UPREL*XNORM+VPREL*YNORM+WPREL*ZNORM
C  :::
C ::: GAMMAA IS THE ANGLE BETWEEN THE NORMAL AND RELATIVE VELOCITY
C  :::
         QPART=SQRT(UPREL**2+VPREL**2+WPREL**2)
       GAMMAA=acos(-(UPREL*XNORM+VPREL*YNORM+WPREL*ZNORM)/QPART)
c
C ::: DETERMINE THE POINT (XWALHT,YWALHT,ZWALHT) THE DROP HIT THE WALL.
C ::: DPOINT IS THE NORMAL DISTANCE FROM THE PRESENT DROP TO THE WALL.
C  :::
       DPOINT=(XP(NPN)-XPOINT)*XNORM+(YP(NPN)-YPOINT)*YNORM+
      1       (ZP(NPN)-ZPOINT)*ZNORM
       DPOQCG=DPOINT/(QPART*cos(GAMMAA))
      XWALHT    =XP(NPN)+DPOQCG*UPREL
      YWALHT    =YP(NPN)+DPOQCG*VPREL
      ZWALHT    =ZP(NPN)+DPOQCG*WPREL
c
```

```
        surten=max(stm*tp(npn)+stb,1.0e-06)
        wedrop=rhop*(qdotn**2)*2.0*radp(npn)/surten
c
c       test to determine the nature of the impact
c
        if(wedrop.le.80.0) then
c       weber number after impact
        wedropo=0.67852227*wedrop*(exp((-4.415135e-02)*wedrop))
c       normal velocity after impact
        qdotn2=qdotn*(1.0+sqrt(wedropo/wedrop))
c       velocity components
        up(npn)=uprel-qdotn2*xnorm
        vp(npn)=vprel-qdotn2*ynorm
        wp(npn)=wprel-qdotn2*znorm+wpist
c
c       new location
c
        xp(npn)=xwalht+abs(dpoqcg)*up(npn)
        yp(npn)=ywalht+abs(dpoqcg)*vp(npn)
        zp(npn)=zwalht+abs(dpoqcg)*wp(npn)
c
        distwp=sqrt((xp(npn)-xwalht)**2+(yp(npn)-ywalht)**2+
     *   (zp(npn)-zwalht)**2)
c
        else
C  :::
C ::: THE TANGENTIAL VECTOR ON THE WALL SURFACE IN THE DIRECTION OF
C ::: THE RELATIVE VELOCITY VECTOR IS GIVE BY (XTAN,YTAN,ZTAN)
C  :::
    XTAN=UPREL-QDOTN*XNORM
    YTAN=VPREL-QDOTN*YNORM
    ZTAN=WPREL-QDOTN*ZNORM
        STAN=SQRT(XTAN**2+YTAN**2+ZTAN**2)
     XTAN=XTAN/STAN
     YTAN=YTAN/STAN
     ZTAN=ZTAN/STAN
C  :::
C ::: THE BINORMAL VECTOR B=(T X N) IS IN THE PLANE OF THE SURFACE
C  ::: B=(XBIN,YBIN,ZBIN)
C  :::
    XBIN=YTAN*ZNORM-ZTAN*YNORM
    YBIN=ZTAN*XNORM-XTAN*ZNORM
    ZBIN=XTAN*YNORM-YTAN*XNORM
C  :::
C ::: DETERMINE PSI THE ANGLE RELATIVE TO THE TANGENTIAL VECTOR IN
C ::: THE PLANE OF THE WALL TO MOVE THE DROP. BETA IS THE PARAMETER
C ::: DETERMINED FROM THE ANGLE GAMMAA.
C  :::
        BETA=PI*SQRT(sin(GAMMAA)/(1.0-sin(GAMMAA)))
      XXX=FRAN(0.0)
      YYY=FRAN(0.0)
        PSI=-(PI/BETA)* log(1.0-XXX*(1.0-EXP(-BETA)))
      IF(YYY.GT.0.5) PSI=-PSI
C  :::
```

```
C ::: FIND THE DIRECTION OF THE NEW RELATIVE VELOCITY
C  :::
      COSPSI=cos(PSI)
       SINPSI=sin(PSI)
      XVNEW=XTAN*COSPSI+XBIN*SINPSI
      YVNEW=YTAN*COSPSI+YBIN*SINPSI
      ZVNEW=ZTAN*COSPSI+ZBIN*SINPSI
C  :::
C ::: SET THE NEW RELATIVE VELOCITY AS SOME FRACTION (FRACT) OF THE OLD
C ::: RELATIVE VELOCITY AND UP DATE THE NEW ABSOLUTE VELOCITIES.
C  :::
       FRACT=1.0
      VELNEW=FRACT*QPART
      UP(NPN)=VELNEW*XVNEW
      VP(NPN)=VELNEW*YVNEW
      WP(NPN)=VELNEW*ZVNEW + WPIST
c
c         new location
       DMOVE=2.0*RADP(NPN)
      XP(NPN)=XWALHT+DMOVE*XNORM
      YP(NPN)=YWALHT+DMOVE*YNORM
      ZP(NPN)=ZWALHT+DMOVE*ZNORM
c
    END IF
C  :::
    RETURN
    END
```

```
      subroutine chemprn
      include 'comd.com'
C +++
CROLF.1/88...  PRINCETON COMBUSTION MODEL .....
C ... FROM ABRAHAM ET AL. COMBUSTION & FLAME, VOL. 60, P. 309, 1985.
C +++
c      DIMENSION YY(9),CK(9),A(5),B(5),D(5)
       DIMENSION YY(12),CK(12),A(5),B(5),D(5)
     REAL KCO2,KH2O
        F0(Q)=16.318*Q-18.972
            F1(Q)=11.2213*Q**3-21.8752*Q**2+14.9469*Q-2.654
        F2(Q)=0.9952*Q-0.3514
        DATA EPSIT,ITMAX/1.E-03,90/
         DATA BCO2,ECO2,SCO2/5.86E-06,68353.9,0.9908/
         DATA BH2O,EH2O,SH2O/8.60534E-06,10415.9,0.9894/
       DATA IFUEL,IO2,IN2,ICO2,IH2O,IH2,ICO,INO/
         &1,2,3,4,5,7,11,12/
       DATA CM1, CM2 , CM3 /
       &    8.25,0.142,0.235/
C NOTE: CM1 INCREASED TO FOR PR=0.66. USE 1.9 FOR SHORT SPARK ELSE 1.8
        data taud,hspark/0.,0.3/
        DATA ANUMC,ANUMH,ANUMO/3.,8.,0./
        data BF,EA,SSL1,SSL2,SSL3,ALPHA1,ALPHA2,BETA1,BETA2,ACTEX1,ACTEX2/
          &      1.54e-12,3.0e04,34.22,138.65,1.08,2.18,0.8,0.16,0.22,0.08,1.15/
         data temspk,pspark,gamspk,resid,phispk/0.,0.,0.,0.,0./
       TCHEM = 1.0E-10
       nspark=2
        if (iignl(2).eq.0) nspark=1
C %%% LOCATE THE IGNITION CELL
      IF (NHO.GT.0) GO TO 191
      DO 190 N=1,NSPARK
      DO 180 K=1,NZ
       I4K=(K-1)*NXPNYP
        I4JK=I4K+(JIGNF(N)-1)*NXP
       I4=I4JK+IIGNL(N)
     IF(ZHEAD-Z(I4).LE.HSPARK) GO TO 185
  180 CONTINUE
  185 KSPARK = K
     IF (KSPARK.GE.NZ) KSPARK = NZ-1
     KIGNB(N)=KSPARK
     KIGNT(N)=KSPARK
  190 CONTINUE
  191 CONTINUE
       I4R    = (KIGNB(1)-1)*NXPNYP + (JIGNF(1)-1)*NXP + IIGNL(1)
COMB _______ STORE UNBURNED GAS PARAMETERS FOR IGNITION MODEL ______
      IF (TAUD.NE.0.) GO TO 1000
      PHISPK=0.
      DO 900 K=1,NZ
       I4B=(K-1)*NXPNYP
       DO 800 J=1,NY
         I4=I4B+(J-1)*NXP+1
       DO 700 I=1,NX
       IF(F(I4).EQ.0.) GO TO 700
       DO 200 ISP=1,nsp
```

```
      YY(ISP)=SPD(I4,ISP)/RO(I4)
      CK(ISP)=SPD(I4,ISP)*RMW(ISP)/RO(I4)
 200 CONTINUE
     OXYGN=2.*(CK(IO2)+CK(ICO2))+CK(IH2O)+CK(ICO)+ANUMO*CK(IFUEL)
     HYDRN=2.*(CK(IH2O)+CK(IH2))              +ANUMH*CK(IFUEL)
     CARBN=CK(ICO2)+CK(ICO)                  +ANUMC*CK(IFUEL)
      IF (I4.EQ.I4R) PHISPK=CK(IFUEL)*(2.*ANUMC+0.5*ANUMH)/
    &                (ANUMO*CK(IFUEL)+2.*CK(IO2))
     SUMY=0.
      DO 210 ISP = 4,11
 210 SUMY      = SUMY + YY(ISP)
      if (i4.eq.i4r) resid=sumy
C +++ SAVE RESIDUAL CONCENTRATIONS AT THE TIME OF SPARK IN SPD(NSP)
c     SPD(I4,NSP)= SUMY*RO(I4)
  700 I4=I4+1
 800 CONTINUE
 900 CONTINUE
C +++
     TEMSPK = TEMP(I4R)
     PSPARK = P(I4R)
     GAMSPK = GAMMA(I4R)
C
 1000 CONTINUE
C
C ..... ESTIMATE THE UNBURNED GAS TEMPERATURE .....
C ..... AND LAMINAR FLAME SPEED NEAR THE SPARK CELL .....
C
      TEMPI4 = TEMSPK*(P(I4R)/PSPARK)**(1.-1./GAMSPK)
      SSUBL0 = SSL1 - SSL2*(PHISPK-SSL3)**2
     IF (SSUBL0.LT.1.0) SSUBL0 = 1.0
      ALPHA  = ALPHA1 - ALPHA2*(PHISPK - 1.)
      BETA   =-BETA1 + BETA2*(PHISPK - 1.)
       SSUBL    = SSUBL0*((TEMPI4/298.)**ALPHA)
         &*((P(I4R)/1.013E06)**BETA)*(1.-2.1*RESID)
     IF (SSUBL.LT.1.0) SSUBL = 1.0
       ELT      = 0.1643168*(TKE(I4R)**1.5)/EPS(I4R)
C
     TAUD= CM1*ELT/SSUBL
C
C ..... END SETUP FOR FLAME KERNEL GROWTH MONITORING .....
C
     DO 90 K=1,NZ
      I4B=(K-1)*NXPNYP
     DO 80 J=1,NY
       I4=I4B+(J-1)*NXP+1
     DO 70 I=1,NX
     IF(F(I4).EQ.0.) GO TO 70
C +++
C +++ CONCENTRATIONS  CK, MASS FRACTIONS YY
C +++
     DO 20 ISP=1,11
      YY(ISP)=SPD(I4,ISP)/RO(I4)
      CK(ISP)=SPD(I4,ISP)*RMW(ISP)/RO(I4)
  20 CONTINUE
```

```
      OXYGN=2.*(CK(IO2)+CK(ICO2))+CK(IH2O)+CK(ICO)+ANUMO*CK(IFUEL)
      HYDRN=2.*(CK(IH2O)+CK(IH2))              +ANUMH*CK(IFUEL)
      CARBN=CK(ICO2)+CK(ICO)                  +ANUMC*CK(IFUEL)
      EQPHI=(2.*CARBN+0.5*HYDRN)/OXYGN
C ..... APPROX. TREATMENT FOR PHI>3.0 AND PHI<40. .....
        BOT=2.*ANUMC+0.5*ANUMH-3.*ANUMO
      FUEL= 0.
       IF (EQPHI.GE.3.0) FUEL=(2.*CARBN+0.5*HYDRN-3.*OXYGN)/BOT
      CARBN=CARBN-ANUMC*FUEL
      HYDRN=HYDRN-ANUMH*FUEL
      OXYGN=OXYGN-ANUMO*FUEL
C
C ..... ITERATE TO FIND EQUILIBRIUM SPECIES DENSITIES .....
C ..... USE COCO2 RATIO FROM NASA CODE FIT AS INITIAL GUESS ...
C
      IPHI=EQPHI
      IF (IPHI.EQ.0) COCO2=F0(EQPHI)
      IF (IPHI.EQ.1) COCO2=F1(EQPHI-1.)
      IF (IPHI.GT.1) COCO2=F2(EQPHI)
      COCO2=2.*EXP(COCO2)
     COCO0=COCO2
      5 EAA=1.987*TEMP(I4)
       C20=0.
      ECEA=ECO2/EAA
      IF (ECEA.GT.50.) GO TO 6
C ... KCO2 = EQUILIB. CONSTANT FOR CO + .5O2 = CO2 .....
        KCO2=BCO2*(TEMP(I4)**SCO2)*EXP(ECEA)
        C20=2./(KCO2*KCO2*RO(I4))
C ... KH2O = KCO2 / KH2O' (KH2O' EQ. CONST. FOR H2 + 0.5O2 = H2O ) ..
      6 KH2O=BH2O*(TEMP(I4)**SH2O)*EXP(EH2O/EAA)
      A(5)=KH2O*(CARBN-OXYGN)
        A(4)=CARBN*(2.*KH2O+1.)+0.5*HYDRN-OXYGN*(KH2O+1.)
       A(3)=2.*CARBN+0.5*HYDRN-OXYGN+KH2O*C20
       A(2)=(KH2O+1.)*C20
      A(1)=C20
      B(5)=A(5)
      D(5)=B(5)
C .. SOLVE QUARTIC EQUATION FOR CO-CO2 RATIO WITH NEWTON POLY. SOLVER -
      DO 8 ICONC=1,ITMAX
      DO 7 LL=1,4
      L=5-LL
       B(L)=A(L)+COCO2*B(L+1)
     7 D(L)=B(L)+COCO2*D(L+1)
       COC21=COCO2-B(1)/D(2)
     IF (ABS(COC21-COCO2).LT.EPSIT*COCO0) GO TO 9
     COCO2=COC21
   8 IF (COCO2.LT.0.) COCO2=-COCO2
     ERR0=0.
       WRITE(6,14) ITMAX,TEMP(I4)
   14 FORMAT(1H ,2X,'CO-CO2 ITERATION FAILED AFTER',I5,' ITERATIONS',
     $' TEMPERATURE',G10.4)
     COCO2=COCO0
C ... COMPUTE LOCAL EQUILIBRIUM COMPOSITION, YY'S .....
     9 H2O=0.5*HYDRN/(1.+KH2O*COCO2)
```

```
      CO2=CARBN/(1.+COCO2)
      YY(IH2O)=H2O*MW(IH2O)
      YY(ICO2)=CO2*MW(ICO2)
      YY(ICO)=COCO2*CO2*MW(ICO)
       YY(IH2)=H2O*KH2O*COCO2*MW(IH2)
       YY(IO2)=1.-(YY(IH2O)+YY(ICO2)+YY(ICO)+YY(IH2)+YY(IN2))
       IF (EQPHI.GE.2.) YY(IO2)=0.5*C20*MW(IO2)/(COCO2*COCO2)
       YY(IFUEL)=1.-(YY(IO2)+YY(IH2O)+YY(ICO2)+YY(ICO)+YY(IH2)+YY(IN2))
c
      DELTS  = (T-T1IGN)/TAUD
      FACSPK = 1.-EXP(-DELTS)
C ... FIND CHARACTERISTIC REACTION TIME, TAUCHM .....
      CM23   = CM2/CM3
     DELYPS = 0.
      DO 55 ISP = 4,11
  55 DELYPS = DELYPS + SPD(I4,ISP)/RO(I4)
cresidDELYPS = DELYPS - SPD(I4,NSP)/RO(I4)
c      dypsav=delyps
     DELYPS = DELYPS - resid
      DELYFO = (SPD(I4,IFUEL)+SPD(I4,IO2))/RO(I4)-(YY(IFUEL)+YY(IO2))
     DELYPS = ABS(DELYPS)
     DELYFO = ABS(DELYFO)
      FACPHI = 1.0E-20
     IF (DELYFO.NE.0..AND.DELYPS.NE.0.) FACPHI = CM23*DELYPS/DELYFO
       TAUTRB = CM2*TKE(I4)/EPS(I4)
CROLF IF (FACPHI.LT.1..AND.DELYFO.NE.0.) TAUTRB = TAUTRB/FACPHI
    IF (FACPHI.LT.1..AND.DELYFO.NE.0..AND.DELYPS.NE.0.)
    1 TAUTRB = TAUTRB/FACPHI
C ... LAMINAR FLAME KINETIC TIME .....
       EQPHI=CK(IFUEL)*(2.*ANUMC+0.5*ANUMH)/
     &       (ANUMO*CK(IFUEL)+2.*CK(IO2))
      BETA   =-BETA1 + BETA2*(EQPHI - 1.)
         PREEXP  = BF*TEMP(I4)*((1.013E06/P(I4))**(1.+2.*BETA))
CKUO   PREEXP  = BF*TEMP(I4)*((1.013E06/P(I4))**0.75)
       ACTEXP  = (1.+ACTEX1*ABS(EQPHI-ACTEX2))*EA/(1.987*TEMP(I4))
      taulam = 0.
       if (abs(actexp).le.200.)
    &TAULAM = PREEXP*EXP(ACTEXP)
        TAULAM  = 0.62*TAULAM/(1.-2.1*RESID)**2
c
     TAUCHM = TAULAM + TAUTRB*FACSPK
C ..... FIRST ORDER ACCURATE STIFF SCHEME .....
      FACEXP = 1.-EXP(-DT/TAUCHM)
      DO 60 ISP=1,11
      RRATE       = -(SPD(I4,ISP) - RO(I4)*YY(ISP))*FACEXP
      SPD(I4,ISP) = SPD(I4,ISP) + RRATE
      DECHEM      =  - RRATE*HTFORM(ISP)*RMW(ISP)/RO(I4)
     DECHK       = ABS(DECHEM/SIE(I4))
     SIE(I4)     = SIE(I4) + DECHEM
     TCHEM       = max (TCHEM,DECHK)
C    ..... END COMBUSTION MODEL .....
  60 CONTINUE
C
```

```
C ..... EXTENDED ZELDOVICH NOX MODEL .....
C ... FROM J.B. HEYWOOD, PROG. ENERGY COMB. SCI., VOL. 1, P. 135, 1976
C
      NO = 1
      IF (NO.EQ.0) GO TO 70
        TA=TEMP(I4)*0.001
       TALOG= log(TA)
C  EQUILIBRIUM CONSTANTS FROM M&M GMR-4361:
         QK1      = 0.794709* log(TA)-113.208/TA+3.16837-0.443814*TA
     1          +2.69699E-02*TA**2
         QK2      = 0.431310* log(TA)- 59.655/TA+3.50335-0.340016*TA
     1          +1.58715E-02*TA**2
         QK4      = 0.990207* log(TA)- 51.792/TA+0.99307-0.343428*TA
     1          +1.11668E-02*TA**2
         QK5      = 0.652939* log(TA)+  9.823/TA-3.93033-0.163490*TA
     1          +1.42865E-02*TA**2
      QK1   = EXP(QK1)
      QK2   = EXP(QK2)
      QK4   = EXP(QK4)
      QK5   = EXP(QK5)
C     NOW DO NO KINETICS
      OXYGEN = ABS(SPD(I4,IO2))*RMW(IO2)
       XNITRO = ABS(SPD(I4,IN2))*RMW(IN2)
      HYDROG = ABS(SPD(I4,IH2))*RMW(IH2)
        QKNO   = 4.4742*EXP(-75.677/TA)
     QKO2N2 = SQRT(QK1*QK2*OXYGEN*XNITRO)
      ALFAP  = QKNO*RMW(INO)/QKO2N2
       ALFA   = SPD(I4,INO)*ALFAP
     SQK1N2 = SQRT(QK1*XNITRO)
      RR1    = 1.626E13*QKO2N2*SQK1N2/QKNO
        RR2     = 6.625E09*TEMP(I4)*EXP(-3150./TEMP(I4))*SQK1N2*OXYGEN
      RR3    = 4.216E13*SQRT(QK1*XNITRO*OXYGEN*HYDROG/QK5)
        FORWD  = DT*2.*MW(INO)*RR1/(1.+ALFA*RR1/(RR2+RR3))
     TOP   = SPD(I4,INO)+FORWD
        BOT     = 0.5*(1.+SQRT(1.+4.*TOP*FORWD*ALFAP**2))
      SPD(I4,INO) = TOP/BOT
CROLF ..... END NOX MODEL .....
   70 I4=I4+1
  80 CONTINUE
  90 CONTINUE
    RETURN
    END
```

REPORT DOCUMENTATION PAGE

Form Approved
OMB No. 0704-0188

1. AGENCY USE ONLY (Leave blank)	2. REPORT DATE	3. REPORT TYPE AND DATES COVERED
	March 1992	Interim Contractor Report

4. TITLE AND SUBTITLE

Three–Dimensional Modeling of Diesel Engine Intake Flow, Combustion and Emissions

5. FUNDING NUMBERS

WU–778–34–2A
G–NAG3–1087

6. AUTHOR(S)

R.D. Reitz and C.J. Rutland

7. PERFORMING ORGANIZATION NAME(S) AND ADDRESS(ES)

University of Wisconsin–Madison
Engine Research Center
1500 Johnson Drive
Madison, Wisconsin 53706

8. PERFORMING ORGANIZATION REPORT NUMBER

None

9. SPONSORING/MONITORING AGENCY NAMES(S) AND ADDRESS(ES)

U.S. Department of Energy
Office of Conservation
Washington, DC 20545

10. SPONSORING/MONITORING AGENCY REPORT NUMBER

NASA CR–189126
DOE/NASA/1087–1

11. SUPPLEMENTARY NOTES

Prepared under Interagency Agreement DE–A101–91CE50306. Project Manager, William T. Wintucky, Propulsion Systems Division, NASA Lewis Research Center, (216) 433–3406.

12a. DISTRIBUTION/AVAILABILITY STATEMENT

Unclassified - Unlimited
Subject Category 07
DOE Category UC–336

12b. DISTRIBUTION CODE

13. ABSTRACT ***(Maximum 200 words)***

A three–dimensional computer code (KIVA) is being modified to include state-of-the-art submodels for diesel engine flow and combustion: spray atomization, drop breakup/coalescence, multi-component fuel vaporization, spray/wall interaction, ignition and combustion, wall heat transfer, unburned HC and NOx formation, soot and radiation and the intake flow process. Improved and/or new submodels which have been completed are: wall heat transfer with unsteadiness and compressibility, laminar-turbulent characteristic time combustion with unburned HC and Zeldo'vich NOx, and spray/wall impingement with rebounding and sliding drops. Results to date show that adding the effects of unsteadiness and compressibility improves the accuracy of heat transfer predictions; spray drop rebound can occur from walls at low impingement velocities (e.g., in cold-starting); larger spray drops are formed at the nozzle due to the influence of vaporization on the atomization process; a laminar-and-turbulent characteristic time combustion model has the flexibility to match measured engine combustion data over a wide range of operating conditions; and finally, the characteristic time combustion model can also be extended to allow predictions of ignition. The accuracy of the predictions is being assessed by comparisons with available measurements. Additional supporting experiments are also described briefly. To date, comparisons with measured engine cylinder pressure and heat flux data have been made for homogeneous charge, spark-ignited and impression-ignited engines, and also limited comparisons for diesel engines. The model results are in good agreement with the experiments.

14. SUBJECT TERMS

Combustion; Diesel engine; KIVA; Combustion modeling; Diesel engine combustion; Intake flow modeling; Engine intake flow

15. NUMBER OF PAGES

68

16. PRICE CODE

A04

17. SECURITY CLASSIFICATION OF REPORT	18. SECURITY CLASSIFICATION OF THIS PAGE	19. SECURITY CLASSIFICATION OF ABSTRACT	20. LIMITATION OF ABSTRACT
Unclassified	Unclassified	Unclassified	